

SUPPORTING ONLINE MATERIAL

Materials and Methods

In vitro CCA addition assays. His-tagged versions of the CCA-adding enzymes from human (13), *E. coli* (14), and *S. shibatae* (15) were expressed in *E. coli* strain BL21(DE3) and purified using the QIAexpress Ni-NTA Fast Start kit (Qiagen) under native conditions using the manufacturer's protocol. Unlabeled RNA substrates were *in vitro* transcribed using the MAXIscript kit (Ambion) and gel purified. To assay if the RNAs are substrates for the CCA-adding enzyme, 5 pmol of RNA was incubated in a 10 µl reaction containing 100 mM glycine, pH 9.0, 10 mM MgCl₂, 1 mM DTT, 50 µM ATP, 50 µM CTP, 0.05 µM [α -³²P] CTP or [α -³²P] ATP, and 50 ng of purified protein. Reactions were incubated at 37 degrees (human or *E. coli* enzymes) or 70 degrees (*S. shibatae* enzyme) for 30 minutes (unless otherwise indicated). The sequences of all RNA substrates and Northern probes are provided in **Table S5**.

In vitro decay assays. *In vitro* decay assays were performed using substrates that had a single radioactive phosphate on their 5' ends. Decay assays using HeLa nuclear extracts were performed as previously described (30). *E. coli* RNase R was obtained from Epicentre Biotechnologies and decay assays were performed using 20 U of enzyme according to the manufacturer's protocol. Yeast Rrp44 was purified as previously described (27) and yeast Xrn1 was obtained from New England Biolabs. Assays were carried out in 30 µl reaction mixtures containing 10 µM Tris-HCl, pH 8.0, 75 mM NaCl, 100 µM MgCl₂, and 1 mM β -mercaptoethanol.

Northern blots and 3' RACE using miRNA Cloning Linker 1 or 3 (Integrated DNA Technologies) were performed as previously described (9).

Multiplex deep sequencing of 3' ends of yeast tRNAs.

Replicates of yeast strains were grown in YPD medium at 28°C until OD₆₀₀ ~1.5 and then shifted to 37°C. At the indicated time points after shift, 2 mL of culture was harvested, pelleted, rinsed with 1 mL of cold sterile water, pelleted, and frozen on dry ice. RNA was purified from cells using hot phenol as previously described (22).

Yeast strains used in this study:

Strain name (Derivative)	Genotype	Source
JMW 007	BY4741	Whipple et al. 2011
AA0527 (JMW 009)	BY4741 <i>trm8</i> -Δ:: <i>natMX</i> <i>trm4</i> -Δ:: <i>kanMX</i>	Alexandrov et al. 2006
JMW 119	BY4741 <i>trm44</i> -Δ:: <i>natMX</i> <i>tan1</i> -Δ:: <i>kanMX</i>	Whipple et al. 2011
JMW 316	JMW 119 <i>sup61</i> -Δ:: <i>bleR ade2</i> :: <i>tS(CGA)</i> <i>G₅₁:C₆₃</i>	Whipple et al. 2011
JMW 510	BY4741 <i>met22</i> -Δ:: <i>hphMX</i>	This study
JMW 561	JMW 119 <i>sup61</i> -Δ:: <i>bleR ade2</i> :: <i>tS(CGA)</i> <i>U₆:A₆₇</i>	Whipple et al. 2011
JMW 1251	JMW 119 <i>sup61</i> -Δ:: <i>bleR ade2</i> :: <i>tS(CGA)</i> <i>C₆:G₆₇</i> <i>G₅₁:C₆₃ G₂:C₇₁</i>	Whipple et al. 2011
ISC 725	BY4742 <i>xrn1</i> -Δ:: <i>bleR</i>	This study
ISC 850	BY4741 <i>trm44</i> -Δ:: <i>natMX tan1</i> -Δ:: <i>kanMX xrn1</i> -Δ:: <i>bleR</i>	Whipple et al. 2011
LY 1729	<i>MATA trm44</i> -Δ:: <i>natMX tan1</i> -Δ:: <i>kanMX met22</i> -Δ:: <i>hphMX</i>	Chernyakov et al. 2008

The overall sequencing approach used is diagrammed in **Fig. S16**. A pre-adenylated oligo (miRNA Linker 3, IDT; 5'-rAppTTAACCGCGATTCCAG/3ddC/) was ligated to the 3' ends of 1.5 µg of total RNA using the truncated form of T4 RNA Ligase 2 (New England Biolabs). Ligation reactions were incubated at room temperature for 2 hr followed by a phenol/chloroform extraction and ethanol precipitation. Reverse

transcription was then performed using Superscript III (Invitrogen) as per the manufacturer's instructions and 5 pmol of primer complementary to the 3' linker sequence (5'-GACTAGCTGGAATT CGCGTTAAA). cDNAs were amplified by PCR using AmpliTaq DNA Polymerase (Applied Biosystems).

To sequence the 3' ends of the endogenous tRNA^{Ser(CGA)} and tRNA^{Ser(UGA)} transcripts (due to their high similarity, this sequencing approach can not distinguish between them), the following forward (5'- CAAGCAGAAGACGGCATACGAGGxxxxxxGGCTCTGCCCGCGCTGG, where xxxxxxxx is a unique 7-nucleotide barcode for each RNA prep so that multiple samples can be run together in a single lane of an Illumina flow cell) and reverse (5'- AATGATA CGGCGACCACCGAGGACTAGCTGGAATT CGCGTTAAA) primers were used. These forward and reverse primers were also used to amplify the U₆:A₆₇ tRNA^{Ser(CGA)} variant in **Fig. 4B** and **Fig. S17B** – however, only reads that contained the A₆₇ mutation were included in the downstream analysis.

To sequence the 3' ends of the G₅₁:C₆₃, C₆:G₆₇, G₂:C₇₁ tRNA^{Ser(CGA)} variant or the G₅₁:C₆₃ tRNA^{Ser(CGA)} variant, the following forward (5'- CAAGCAGAAGACGGCATACGAGGxxxxxxGCGGGTTCAAATCCCGC, where xxxxxxxx is a unique 7-nucleotide barcode) and reverse (5'- AATGATA CGGCGACCACCGAGGACTAGCTGGAATT CGCGTTAAA) primers were used to avoid amplification of the endogenous tRNA^{Ser(UGA)} loci.

The 7-nucleotide barcodes used were:

ACTGCGC	TCGTCAG	ATCGACG	CTCACAT
ATATCAC	TGTACGC	AGAGTAG	CTCTGCA
ATGCTAC	TGTGCAG	AGTCGAG	ACGTAGC

CACGTCA	AGTATAC	TCGTGTC	ATAGAGC
CATCAGA	TAGCACG	AGATATC	TGATGAC
CGAGACA	ACACGAC	TAGTCGC	ACAGCTG
CGCTCGT	ATCAGAC	TCTAGAC	ATGCATG
CTAGTGA	CGTCTCA	AGTCAGC	TACGTCG
TAATATG	CGTGTGT	TACGAGC	TAGATAG
TATAGCG	CGCATGA	TCGATGC	TGAGTGC
TATCATC	CGACAGT	TGCTCTC	TATGTAC
TCACAGC	AGCTGCG	CAGTGCT	

PCR reactions were incubated at 94° for 2 min, followed by 21 cycles of 94° for 15 sec, 58° for 30 sec, and 72° for 30 sec. All PCR reactions were then combined in one tube and extracted with phenol/chloroform and ethanol precipitated. Using a 2% low melting point agarose gel, the PCR products (~110 to 120 bp) were purified and then cleaned up using a phenol extraction, followed by a phenol/chloroform extraction, followed by a chloroform extraction. The purified DNA was resuspended in water and subjected to deep sequencing using the Illumina HiSeq 2000 Sequencing System and the following sequencing primer (5'-CCGAGGACTAGCTGGAATT CGCGGTTAAA). 58 nucleotide reads from the 3' ends of each transcript were obtained. At least three biological replicates were performed for each strain/time point as shown in **Tables S1-4**. This required the use of multiple sequencing lanes.

The resulting sequencing files were processed by collapsing identical reads and reverse complementing the sequences (as this sequencing strategy actually sequences the reverse complement of a given transcript). The reads were then separated into the individual libraries by only using reads that contained perfect 7-nucleotide barcodes and perfect gene-specific forward primer sequences (the underlined regions in the primer).

For the CCACCA addition analysis (**Table S1**), we only included sequences that were represented by 2 or more reads in the downstream analysis. For the tRNA^{Ser(CGA)} variants, however, we included all reads as these libraries generally had much lower overall read counts (**Table S2**). To calculate the percentage of reads that ended in an extended CCA motif in a given sample, we used the following formula:

$$\frac{\text{\# of reads ending in CCAC, CCACC, or CCACCA}}{\text{\# of reads ending in CCA}} \times 100$$

Although we did detect a handful of reads ending in CCACCCAC, CCACCCACC, or CCACCCACCA (**Tables S1 and S2**), these reads were not included in the analysis.

For the poly(A) tail analysis (**Tables S3 and S4**), we only included sequences that were represented by 10 or more reads in the downstream analysis. For libraries with low overall read counts (*xrn1*-Δ Replicates #2, 3 and the tRNA^{Ser(CGA)} variants), we included sequences that were represented by 2 or more reads in the analysis. To calculate the percentage of reads ending in polyadenylated CCA motifs in a given sample, we used the following formula:

$$\frac{\text{\# of reads ending in CCAA, CCAAA, ..., CCA}_{11}, \text{ or CCA}_{12}}{\text{\# of reads ending in CCA}} \times 100$$

Due to the length of our sequencing reads, only transcripts with 12 or fewer A's were included in our analysis as a complete 7-nt barcode would not be sequenced if the transcript ended in 13 or more A's. Although we did detect tRNAs with up to 19 A's on

their 3' ends (data not shown), all sequences with more than 12 A's were not included in our analysis as we could not unambiguously assign them to their proper library.

Supporting Text

CCACCA addition requires isomerization of the tRNA acceptor stem

Only those MEN β tRNA-like small RNA homologs that have unstable acceptor stems were targets for CCACCA addition *in vitro* (Fig. 2D) or *in vivo* (Fig. S1 and fig. S7). However, the presence of instability is not sufficient to generate a CCACCA target, as a mouse mascRNA mutant (Mut 7, Fig. S8A) that has a C-A mismatch in its acceptor stem remained a CCA target (Fig. S8, B and C). Other single point mutations in mascRNA (Mut 5-9, Fig. S8A) also had no effect on the specificity of the *E. coli* (Fig. S8B) or human (Fig. S8C) CCA-adding enzymes. Introduction of four mutations (Mut 10, Fig. S8A), all located at the end of the acceptor stem, was sufficient to convert mascRNA from a CCA to a CCACCA target *in vitro* (Fig. S8, D and E). A similar transcript (Mut 11, Fig. S8A) containing three mutations but no predicted instability only had CCA added to its 3' end (Fig. S8, D and E), indicating that both instability and specific nucleotides at the end of the acceptor stem were required for CCACCA addition. The distal base pairs of the tRNA acceptor stem are critical for the accuracy of the genetic code as this structure commonly contains identity elements that determine which amino acid will be used to charge the tRNA (31, 32).

To address how the CCA-adding enzyme monitors nucleotide identity at specific positions in the acceptor stem, we generated the Mut 10A mascRNA transcript, which is identical to the Mut 10 RNA except that the C-A mismatch has been swapped across the stem (Fig. S8A). Unlike the Mut 10 substrate, the Mut10A transcript was a CCA target (Fig. S8, F and G). Thus, the CCA-adding enzyme either requires specific nucleotides at the swapped positions or these nucleotides need to form base pairs with other nucleotides

in an alternative RNA conformation for CCACCA addition to occur. In support of the latter, we recognized that after the first CCA is added, the instability in the acceptor stem would facilitate RNA isomerization, such that the right side of the acceptor stem is shifted by three nucleotides (Fig. 2F). The A of the CCA sequence would thus be the new discriminator base and be positioned in the enzyme's catalytic pocket, ready to undergo a second round of CCA addition using the well-established polymerization mechanisms (8, 17-19).

Pursuing this model, the mascRNA Mut 10, but not Mut 10A, transcript can form a base pair in the shifted conformation between nucleotide 3 and the last encoded nucleotide (the original discriminator base) (Fig. S8A). Therefore, it might be possible to convert the Mut 10A transcript to a CCACCA target by mutating the last encoded nucleotide to a U (Mut 10AD, Fig. S8A), thus establishing an A-U base pair in the shifted conformation. Indeed, the Mut 10AD construct was a CCACCA target (Fig. S8, F and G), providing strong support for the RNA isomerization model (Fig. 2E). Interestingly, additional mutational analysis revealed that CCACCA addition can occur even when a base pair can not form between nucleotide 3 and the last encoded nucleotide (Fig. S9). In particular, CCACCA addition to the Mut 10A construct occurs if the end of the acceptor stem is further weakened by the presence of a G-U wobble base pair (Mut 10AU, Fig. S8A and fig. S9E). This is likely because the shifted conformation of the Mut10AU, but not the Mut10A, substrate is predicted to be thermodynamically more stable than the non-shifted conformation. We, therefore, conclude that CCACCA addition requires the transcript to isomerize to a shifted conformation that is, at minimum, of similar predicted stability as the non-shifted conformation.

Combining the results from all of the mutational analysis suggests rules for addition of CCACCA by the CCA-adding enzyme. For CCACCA addition, the RNA must have (1) an unstable acceptor stem, which allows isomerization; (2) guanosines at the first and second positions of the RNA, which form base pairs with the Cs of the first CCA in the shifted conformation; and (3) the ability to isomerize to a stable shifted conformation, e.g. due to a base pair between the third nucleotide and the last encoded nucleotide. We tested and confirmed these rules by mutating the mouse MEN β tRNA-like small RNA, converting it from a CCACCA to a CCA target (Fig. S10), and by defining a minimal set of mutations that convert the canonical tRNAs used in Fig. S5 to CCACCA targets (Fig. S11). In human, 238 annotated tRNAs begin with GG and 66 of these can form a base pair between nucleotide 3 and the last encoded nucleotide (35 form a G-C or A-U base pair, 31 a G-U wobble).

Supplementary Figure Legends

Fig. S1. CCACC(A) is added to the 3' end of the human and mouse MEN β tRNA-like small RNA transcripts. The 3' end of the MEN β tRNA-like small RNA was cloned using a ligation-based approach (3' linker oligo is designated) and RNA from human HeLa cervical carcinoma cells (**A**), mouse C2C12 myoblast cells (**B**), or mouse EpH4-A6 mammary epithelial cells transformed by ErbB2 over-expression (33) (**C**). * denotes a common nucleotide modification site observed in mscRNA (9) and several of the cDNA clones.

Fig. S2. Purification and validation of His-tagged CCA-adding enzymes from all three kingdoms of life. (A to C) His-tagged versions of the CCA-adding enzymes from human (**A**), *E. coli* (**B**), and *S. shibatae* (**C**) were expressed and purified from *E. coli*. 5 µl of each fraction was loaded on a SDS-PAGE gel that was subsequently stained with Coomassie blue. Eluate 2 of each prep was used for all subsequent *in vitro* CCA addition assays. **(D to F)** *In vitro* CCA addition assays using a threonine tRNA as a substrate to verify the specificity of the purified enzymes. The unlabeled tRNA substrates ended in CCA, CC, C or simply the discriminator base (designated No CCA) and were incubated with the CCA-adding enzymes from human (**D**), *E. coli* (**E**), or *S. shibatae* (**F**) in the presence of an excess of cold CTP and ATP as well as a trace amount of either [α -³²P] CTP or [α -³²P] ATP. The reactions were then run on 6% polyacrylamide gels and exposed to a PhosphorImager screen. As the input RNA substrates are not labeled, a band is only observed when the CCA-adding enzyme incorporated the hot nucleotide onto the 3' end of the transcript. In (**F**), CTP reactions were incubated for only 5 min.

Fig. S3. CCACC(A) is added to the 3' end of the MEN β tRNA-like small RNA *in vitro*. (A) *In vitro* CCA addition assays using a threonine tRNA (top), the human MEN β tRNA-like small RNA (middle), or the mouse MEN β tRNA-like small RNA (bottom). The unlabeled substrates ended in the discriminator base (designated No CCA) or CCA and were incubated with the *E. coli* enzyme in the presence of an excess of cold CTP and ATP as well as a trace amount of either [α -³²P] CTP or [α -³²P] ATP. As expected, the threonine tRNA with CCA already on its end was unable to accept any additional nucleotides. In contrast, both the human and mouse MEN β tRNA-like transcripts with CCA already on their 3' ends were efficiently extended. (B) *In vitro* transcribed mouse MEN β tRNA-like small RNA lacking CCA at its 3' end was used as a substrate for the *E. coli* CCA-adding enzyme. A ligation-based 3' RACE approach (3' linker oligo is designated) was then used to clone the 3' ends of the *in vitro* reaction products.

Fig. S4. CCA-adding enzymes from all three kingdoms of life are able to build and repair a 3'-terminal CCACCA motif. (A) Generation of mouse mmascRNA (denoted mmascRNA) chimeras in which one of the arms was swapped with that of the mouse MEN β tRNA-like small RNA. All sequences derived from mmascRNA are in uppercase, whereas all sequences derived from the MEN β tRNA-like small RNA are in lowercase. (B) *In vitro* transcribed mmascRNA or mmascRNA Mut 1 lacking CCA at its 3' end were used as substrates for the *E. coli* CCA-adding enzyme. A ligation-based 3' RACE approach (3' linker oligo is designated) was then used to verify that the *E. coli* enzyme adds CCACCA to the 3' end of the mmascRNA Mut 1 transcript *in vitro*. (C) Swapping the mmascRNA acceptor stem with that of the mouse MEN β tRNA-like small RNA

(Mut 1) converts the transcript to a CCACCA target for the *E. coli* enzyme. **(D to F)** Wild-type mouse mascRNA or mmascRNA Mut 1 substrates with different 3' termini were incubated *in vitro* with the CCA-adding enzymes from human **(D)**, *E. coli* **(E)**, or *S. shibatae* **(F)**. All three enzymes are able to repair the 3'-terminal CCA or CCACCA motifs on mmascRNA and mmascRNA Mut 1, respectively. Consistent with a previous report that demonstrated that the *E. coli* CCA-adding enzyme is able to add A to the 3' end of any RNA ending in CC *in vitro* (34), we observed that the *E. coli* CCA-adding enzyme efficiently adds A to the mmascRNA substrate ending in CCACC.

Fig. S5. Swapping the acceptor stems of canonical tRNAs with that of the MEN β tRNA-like small RNA converts the transcripts to CCACCA targets *in vitro*. Wild-type tRNAs or ones with their acceptor stem swapped with that of mouse mascRNA or mouse MEN β tRNA-like small RNA [denoted at top in **(A)**] were used as substrates. RNA substrates either lacked CCA on their 3' ends **(A)** or had various 3' termini as denoted at the top **(B)**. Whereas wild-type tRNAs and tRNAs with the mascRNA acceptor stem were substrates for CCA addition, all tRNAs tested that had the MEN β acceptor stem were substrates for CCACCA addition.

Fig. S6. Conservation of mascRNA and the MEN β tRNA-like small RNA across species. The acceptor stems of the two transcripts are shaded in blue. Compared to mascRNA, the right side of the MEN β tRNA-like small RNA acceptor stem has been very poorly conserved throughout evolution, suggesting that it may be becoming a pseudogene.

Fig. S7. The MEN β tRNA-like small RNA is a CCA target and stable transcript in African Green Monkey COS7 cells. (A) Northern blot analysis using 15 µg of total RNA from human HeLa cells, human MCF7 cells, or African Green Monkey COS7 cells. Unlike the human homolog, expression of the African Green Monkey MEN β tRNA-like small RNA was easily detected. U6 snRNA was used as a loading control. (B) The 3' ends of mascRNA and the MEN β tRNA-like small RNA were cloned using a ligation-based approach (3' linker oligo is designated) and RNA from COS7 cells.

Fig. S8. The tRNA acceptor stem is isomerized to allow for CCACCA addition. (A) Predicted secondary structures of the acceptor stems from wild-type and mutant mouse mascRNA transcripts. Mut 1 is equivalent to the acceptor stem of the mouse MEN β tRNA-like small RNA and was used as a guide to generate the other mutants. Nucleotides in blue are conserved between mouse mascRNA and the mouse MEN β tRNA-like small RNA, while nucleotides in black or red are specific to mascRNA or the MEN β transcript, respectively. (B to G) *In vitro* assays using the *E. coli* or human CCA-adding enzyme (as noted at the top of each figure part) were performed using WT or mutant mascRNA substrates. We obtained highly similar results with both enzymes, indicating that the human and *E. coli* enzymes recognize the same features in the tRNA acceptor stem to determine whether to add CCA or CCACCA.

Fig. S9. A base pair between the third nucleotide and the discriminator base in the shifted conformation is not absolutely required for CCACCA addition. (A) In contrast to Fig. S8 where we swapped the mouse mascRNA acceptor stem with that of the mouse MEN β tRNA-like small RNA, here we swapped the mouse mascRNA

acceptor stem with that of the human MEN β tRNA-like small RNA (generating the Mut 14 substrate). The human MEN β acceptor stem has no mismatches but does have multiple G-U wobble base pairs at the end of the stem. We then generated additional mutants to determine which nucleotide changes are required to convert mascRNA from a CCA to a CCACCA target. **(B)** Wild-type mouse mascRNA or the Mut 14-17 substrates were incubated with the *E. coli* CCA-adding enzyme. Of particular interest, CCACCA was efficiently added to the 3' end of the Mut 16 substrate despite the fact that it can not form a base pair between the third nucleotide and the discriminator base (it instead forms a C-U mismatch). **(C)** Analogous to the strategy used to generate the mascRNA Mut 10A and Mut 10AD constructs from Mut 10 in **Fig. S8A**, we swapped the third base pair of Mut 15 across the stem to generate the Mut 15A substrate. Whereas Mut 15 can form a C-G base pair between the third nucleotide and the discriminator base, Mut 15A forms a G-G mismatch and Mut 15AD re-establishes the potential for this base pair. Interestingly, Mut 15, 15A, and 15AD are all efficient substrates for CCACCA addition, likely because the shifted conformations of all three substrates are predicted to be of similar stability as the non-shifted conformations. **(D)** Comparison of the acceptor stems of mascRNA Mut 10A, a CCA target, and Mut 15A, a CCACCA target. There are only three point mutations between the two substrates (denoted in red), which we used as a guide to generate the Mut10AU construct in **Fig. S8A**. **(E)** CCACCA addition to the Mut10A construct can be rescued by the presence of a G-U wobble at the end of the acceptor stem (Mut 10AU).

Fig. S10. Mutational analysis to convert the mouse MEN β tRNA-like small RNA from a CCACCA to a CCA target *in vitro*. **(A)** Predicted secondary structures of the

acceptor stems from the wild-type and mutant mouse MEN β tRNA-like transcripts. Mut 1 is equivalent to the acceptor stem of mouse masCRNA and was used as a guide to generate the other mutants. Below the structures is a chart that describes if each substrate follows the rules for CCA or CCACCA addition and if the prediction matches the experimental data in (B). (B) *In vitro* CCA addition assays using the *E. coli* enzyme. We found that the wild-type mouse MEN β tRNA-like small RNA transcript consistently migrated anomalously (it is expected to run at 63 nucleotides, but generally ran as a doublet at \sim 55 and \sim 60 nucleotides, possibly suggesting different RNA conformations). The addition of a single nucleotide in the D-arm (Mut 2 substrate) had no effect on CCACCA addition but caused the transcript to migrate as a single band at the expected size, so all other mutant substrates also have this change in their D-arms and are thus designated Mut #+D. All mutant substrates followed the rules for CCA versus CCACCA addition with the possible exception of Mut 6+D which was weakly able to accept an additional C when it already had CCA on its end.

Fig. S11. Mutational analysis to convert canonical tRNAs from CCA to CCACCA targets *in vitro*. (A) Predicted secondary structures of the acceptor stems from wild-type and mutant tRNA-Thr-ACY transcripts. Mut 1 and Mut 2 are equivalent to the acceptor stems of mouse masCRNA and the mouse MEN β tRNA-like small RNA, respectively. The MEN β acceptor stem was used as a guide to generate the other mutants. Below the structures is a chart that describes if each substrate follows the rules for CCA or CCACCA addition and if the prediction matches the experimental data. (B) *In vitro* CCA addition assays using the *E. coli* enzyme and wild-type or mutant tRNA-Thr-ACY substrates that lack CCA at their 3' termini. (C) Similar mutational analysis was

performed using a tRNA-Leu-CTY transcript. **(D)** *In vitro* CCA addition assays using the *E. coli* enzyme and wild-type or mutant tRNA-Leu-CTY substrates that lack CCA at their 3' termini. All mutant threonine and leucine tRNAs followed the rules for CCA versus CCACCA addition.

Fig. S12. GG is enriched at the 5' ends of tRNA genes from all three kingdoms of life. The sequences of all tRNA genes (including potential pseudogenes, if present) encoded in the genomes of 16 species were obtained from the Genomic tRNA Database (<http://gtrnadb.ucsc.edu>). As GG is required at the 5' end of a tRNA for CCACCA addition to occur, we analyzed the sequences to determine how common GG is at the 5' end of tRNAs. For each species, the actual number of tRNAs that have a given dinucleotide combination at their 5' end and the corresponding percentage of the total are shown in the # and % columns, respectively. The numbers in red indicate the most abundant 5' end combination in each species. In the Summary table, we combined the data from all 16 species to show that, in general, GG is the most common dinucleotide combination at the 5' ends of tRNAs. One would only expect 6.25% of tRNAs to start with GG if the sequences were completely random. Sequences are from *Arabidopsis thaliana* (Feb 2004), *Caenorhabditis elegans* (Jan 2007), *Drosophila melanogaster* (Release 5 Apr 2006), *Homo sapiens* (hg18 - NCBI Build 36.1 Mar 2006), *Mus musculus* (mm9 July 2007), *Saccharomyces cerevisiae*, *Zea mays* (Version 4a.53), *Escherichia coli* K12, *Haemophilus influenzae*, *Mycobacterium tuberculosis* CDC1551, *Mycoplasma pneumoniae*, *Vibrio cholerae*, *Candidatus Korarchaeum cryptofilum* OPF8, *Methanoscincina acetivorans*, *Nanoarchaeum equitans*, and *Sulfolobus solfataricus*.

Fig. S13. Single point mutations can convert arginine tRNAs from CCA to CCACCA targets *in vitro*. (A) We chose to mutate two unrelated arginine tRNAs that have GG at their 5' ends and the ability to form a base pair between the third nucleotide and the discriminator base. Nevertheless, the wild-type tRNAs have stable acceptor stems, making them targets for CCA addition. Single point mutations were introduced to destabilize the acceptor stem as shown. (B to C) *In vitro* CCA addition assays using the human or *E. coli* CCA-adding enzyme. All of the single point mutations tested were sufficient to efficiently convert the tRNA from CCA to CCACCA addition.

Fig. S14. Single point mutations can convert a cysteine tRNA from a CCA to a CCACCA target *in vitro*. (A) We mutated a wild-type cysteine tRNA by introducing single point mutations that should destabilize the acceptor stem. The last mutant (G2A) creates an unstable acceptor stem but mutates the 5' end of the transcript from GG to GA and was thus expected to remain a target for CCA addition. (B) *In vitro* CCA addition assays using the *E. coli* enzyme. All mutants followed the rules for CCA versus CCACCA addition, including the G2A mutant, which remained a CCA target.

Fig. S15. Mutant tRNAs ending in CCACCA are rapidly degraded *in vitro*. The *in vitro* decay assay in Fig. 3C was repeated using a shorter time course. Radiolabeled wild-type or mutant arginine tRNAs with CCA or CCACCA at their 3' ends, respectively, were incubated in HeLa nuclear extracts for the indicated amounts of time. Arrow denotes a slight accumulation of wild-type tRNAs cleaved in the anticodon loop.

Fig. S16. Multiplex deep sequencing strategy used to analyze the 3' ends of specific tRNAs. (A) Using total RNA isolated from various conditions, a linker oligo (drawn in

brown) is first ligated to the 3' ends, which is subsequently used as a priming site for first-strand cDNA synthesis. A gene-specific forward primer containing a unique barcode is then used for 3' RACE PCR. By combining all of the PCR products from each of the conditions together, multiplex deep sequencing can be performed. The barcodes are then used to determine the source of each read, allowing one to analyze the 3' end of a given tRNA under many conditions. **(B)** Diagram depicting the primers used for 3' RACE PCR on tRNA^{Ser(CGA)}. The gene-specific forward primer hybridizes to a region spanning the variable arm and T-stem.

Fig. S17. Short poly(A) tails are added to mature tRNAs being degraded by RTD *in vivo*. **(A)** In addition to increases in CCACCA addition levels during RTD, we noticed a significant number of mature tRNAs that had a short poly(A) tail added to their CCA end when the transcripts were being actively degraded. A low, but reproducible, level of polyadenylated CCA motifs (defined as CCAA, CCAAA, etc.) was detected on tRNA^{Ser(CGA)} and tRNA^{Ser(UGA)} in a wild type strain grown at 28°C or 37°C (**Table S3**). Upon switching the *trm44*-Δ *tan1*-Δ deletion strain to growth at 37°C, a progressive increase in polyadenylated CCA motifs was observed (41.6 +/- 8.8 fold over wild-type levels at the 6 hr time point), which mirrors the time course of tRNA degradation. Deleting Xrn1 or Met22 rescued this effect. **(B)** As in **Fig. 4B**, we replaced the endogenous tRNA^{Ser(CGA)} gene in the *trm44*-Δ *tan1*-Δ deletion strain with the tRNA^{Ser(CGA)} variants shown. Increasing the structural stability of the tRNAs made the transcripts resistant to polyadenylation and RTD. Error bars represent standard deviation.

Fig. S18. Mature tRNAs ending in CCACCA are efficiently degraded *in vitro*. (A)

Radiolabeled wild-type tRNAs with CCA or CCACCA at their 3' ends (as denoted at top) were incubated with *E. coli* RNase R, a 3'-5' exonuclease, for the indicated amounts of time. **(B)** An arginine tRNA ending in CCACCA, but not CCA, was efficiently degraded by yeast Rrp44 *in vitro*. Degradation is dependent on the 3'-5' exonuclease activity of Rrp44 as a point mutation in the active site (D551N) abrogated this effect. **(C)** Mature tRNAs (radioactively labeled at their 5' end) ending in CCACCA were incubated with yeast Rrp44, yeast Xrn1, or both enzymes for the indicated amounts of time. Increased degradation rates were observed when both 3'-5' and 5'-3' exonucleases were present. As the transcripts are radioactively labeled only at their 5' ends, the degradation intermediates observed in the Rrp44 alone reactions correspond to tRNAs with shortened 3' tails. This suggests that Rrp44 pauses once it nears the double-stranded tRNA acceptor stem. In the Xrn1-deficient strain, we propose that only the extended 3' tail of the transcript would be removed, resulting in a rescue of the phenotype at high temperatures and in the observed decrease in transcripts ending in CCACCA in **Fig. 4A**.

Fig. S19. The CCA-adding enzyme functions in tRNA maturation, repair, and quality control. A primary tRNA transcript in eukaryotes is cleaved by RNase P and RNase Z near its 5' and 3' ends, respectively, to generate a transcript that is recognized by the CCA-adding enzyme (drawn in purple). For a normal tRNA with a stable structure, the CCA-adding enzyme catalyzes the addition of CCA to its 3' end. Once released from the CCA-adding enzyme, the tRNA is recognized by the appropriate aminoacyl tRNA synthetase, which charges it with an amino acid, thus completing the maturation of the tRNA. If the CCA terminus becomes damaged at any point, the CCA-

adding enzyme recognizes the damage and repairs it, thus re-generating a functional tRNA that can be aminoacylated and used by the ribosome. In addition to these roles in tRNA maturation and repair, our work has now shown that the CCA-adding enzyme functions in tRNA quality control. If the tRNA structure becomes destabilized (e.g. because of mistakes during transcription or the lack of post-transcriptional nucleotide modifications) and the other rules are followed, the CCA-adding enzyme recognizes an alternate conformation of the tRNA, such that a second CCA motif is added to the 3' end. Alternatively, a short poly(A) tail can be added to the CCA motif. These structurally unstable tRNAs are then targeted for degradation, preventing potential downstream errors in aminoacylation or translation.

Fig. S20. Identification of two tRNAs that are encoded in the genome as CCACCA targets reveals likely regulatory roles for CCACCA addition. **(A)** In the jakobid protist *Seculamonas ecuadoriensis*, the mitochondrial serine tRNA contains two mismatched base pairs in its acceptor stem (shown in red). Interestingly, these mismatches are corrected post-transcriptionally *in vivo* to generate canonical base pairs (28). The arrows show the nucleotide changes introduced by editing. Leigh and Lang proposed that this occurs by exonucleolytic degradation of the 3' end of the tRNA acceptor stem followed by repair by a hypothetical enzyme whose activity resembles that of the CCA-adding enzyme because nearly all of the inserted nucleotides are either C or A (28). **(B)** *In vitro* CCA addition assays using the human or *E. coli* enzymes. Unlike the fully edited form, the genomic version of the *S. ecuadoriensis* mitochondrial serine tRNA is a CCACCA target. **(C)** As the hypothetical enzyme proposed by Leigh and Lang has never been identified, we instead propose a model in which the CCA-adding enzyme

adds CCACCA to the end of the tRNA, followed by a splicing-like event that removes the three bulged nucleotides. CCACCA addition by the CCA-adding enzyme may, therefore, be critical for the maturation of certain tRNAs. **(D and E)** In the amoeboid protozoan *Acanthamoeba castellanii*, the acceptor stem of the mitochondrial alanine tRNA contains a mismatch between U₃:U₇₀, causing the transcript to be subjected to CCACCA addition *in vitro*. However, this mismatch is corrected to an A-U base pair *in vivo* by a previously identified post-transcriptional RNA editing event (29), generating a functional tRNA that is a CCA target. We, therefore, propose that CCACCA addition serves as a checkpoint that ensures that this mismatch is corrected, an event that is especially critical for this tRNA as the third base pair is a major determinant of alanine aminoacylation specificity in many species.

Supplementary Table Legends

Table S1. Addition of extended CCA motifs to tRNA^{Ser(CGA)} and tRNA^{Ser(UGA)} during RTD. The data used in **Fig. 4A** is shown. For each sample, the total number of reads in the library as well as the number of reads that ended in CCA, CCAC, CCACC, CCACCA, etc. is given. As described in the Materials and Methods, we summed the number of reads ending in CCAC, CCACC, or CCACCA to determine the percentage of reads ending in an extended CCA motifs (Column 14).

Table S2. Stabilizing the structure of tRNA^{Ser(CGA)} inhibits RTD and CCACCA addition. The data used in **Fig. 4B** is shown. For each sample, the total number of reads in the library as well as the number of reads that ended in CCA, CCAC, CCACC, CCACCA, etc. is given. As described in the Materials and Methods, we summed the number of reads ending in CCAC, CCACC, or CCACCA to determine the percentage of reads ending in an extended CCA motifs (Column 14).

Table S3. Addition of poly(A) tails to mature tRNA^{Ser(CGA)} and tRNA^{Ser(UGA)} transcripts during RTD. The data used in **Fig. S17A** is shown. For each sample, the total number of reads in the library as well as the number of reads that ended in CCA, CCAA (denoted 2 A's), CCAAA (denoted 3 A's), CCAAAA (denoted 4 A's), etc. is given. As described in the Materials and Methods, we summed the number of reads ending in 2 to 12 A's to determine the percentage of reads ending in a polyadenylated CCA motif (Column 19).

Table S4. Stabilizing the structure of tRNA^{Ser(CGA)} inhibits RTD and the addition of poly(A) tails. The data used in **Fig. S17B** is shown. For each sample, the total number of reads in the library as well as the number of reads that ended in CCA, CCAA (denoted 2 A's), CCAAA (denoted 3 A's), CCAAAA (denoted 4 A's), etc. is given. As described in the Materials and Methods, we summed the number of reads ending in 2 to 12 A's to determine the percentage of reads ending in a polyadenylated CCA motif (Column 19).

Table S5. Sequences of all RNA substrates and Northern blot probes used. The sequences of all RNA substrates are given as the “No CCA” version. Additional nucleotides (C, CC, CCA, CCAC, CCACC, or CCACCA) were included at the 3' ends of the substrates as indicated in the figures and text. All substrates that start with GG at their 5' ends were transcribed using T7 RNA polymerase, whereas all substrates that start with GA were transcribed using SP6 RNA polymerase.

Supplementary References

30. L. P. Ford, P. S. Bagga, J. Wilusz, *Mol Cell Biol* **17**, 398 (1997).
31. R. Giege, M. Sissler, C. Florentz, *Nucleic Acids Res* **26**, 5017 (1998).
32. M. Ibba, D. Soll, *Annu Rev Biochem* **69**, 617 (2000).
33. V. R. Fantin, M. J. Berardi, L. Scorrano, S. J. Korsmeyer, P. Leder, *Cancer Cell* **2**, 29 (2002).
34. E. Lizano, M. Scheibe, C. Rammelt, H. Betat, M. Morl, *Biochimie* **90**, 762 (2008).

A**HeLa**

hGenomic DNA	GGTGGCACGCCAGCACGGCTGGGCCGGGTTCGAGTCCCCGAGTGTGCTGCTCCAGCT
17 Clones	GGTGGCACGCCAGCACGGCTGGGCCGGGTTCGAGTCCCCGAGTGTGCTGCTCCAGCT CCACCA ctgttaggcaccatcaatc
4 Clones	GGTGGCACGCCAGCACGGCTGGGCCGGGTTCGAGTCCCCGAGTGTGCTGCTCCAGCT CCACCA ctgttaggcaccatcaatc *
	Ligated 3' Linker
2 Clones	GGTGGCACGCCAGCACGGCTGGGCCGGGTTCGAGTCCCCGAGTGTGCTGCTCCAGCT CCACCA ctgttaggcaccatcaatc
1 Clone	GGTGGCACGCCAGCACGGCTGGGCCGGGTTCGAGTCCCCGAGTGTGCTGCTCCAGCT CCACCA ctgttaggcaccatcaatc *
	Ligated 3' Linker
1 Clone	GGTGGCACGCCAGCACGGCTGGGCCGGGTTCGAGTCCCCGAGTGTGCTGCTCCAGCT CCACCA ctgttaggcaccatcaatc *
	Ligated 3' Linker

B**C2C12**

mGenomic DNA	GGCACGCCGCACCTCGGCCAGGGTCAGTCCCTGCAGTACCGTGCCTGCTCT
9 Clones	GGCACGCCGCACCTCGGCCAGGGTCAGTCCCTGCAGTACCG CCACCA ctgttaggcaccatcaatc *
	Ligated 3' Linker
1 Clone	GGCACGCCGCACCTCGGCCAGGGTCAGTCCCTGCAGTACCG CCACCA ctgttaggcaccatcaatc *
	Ligated 3' Linker

C**EpH4-A6**

mGenomic DNA	GGCACGCCGCACCTCGGCCAGGGTCAGTCCCTGCAGTACCGTGCCTGCTCT
1 Clone	GGCACGCCGCACCTCGGCCAGGGTCAGTCCCTGCAGTACCG CCACCA ctgttaggcaccatcaatc *
	Ligated 3' Linker
12 Clones	GGCACGCCGCACCTCGGCCAGGGTCAGTCCCTGCAGTACCG CCACCA ctgttaggcaccatcaatc
2 Clones	GGCACGCCGCACCTCGGCCAGGGTCAGTCCCTGCAGTACCG CCACCA ctgttaggcaccatcaatc
1 Clone	GGCACGCCGCACCTCGGCCAGGGTCAGTCCCTGCAGTACCG CCACCA ctgttaggcaccatcaatc *
	Ligated 3' Linker
4 Clones	GGCACGCCGCACCTCGGCCAGGGTCAGTCCCTGCAGTACCG CCACCA ctgttaggcaccatcaatc *
	Ligated 3' Linker
3 Clones	GGCACGCCGCACCTCGGCCAGGGTCAGTCCCTGCAGTACCG CCACCA ctgttaggcaccatcaatc *
	Ligated 3' Linker

Figure S1

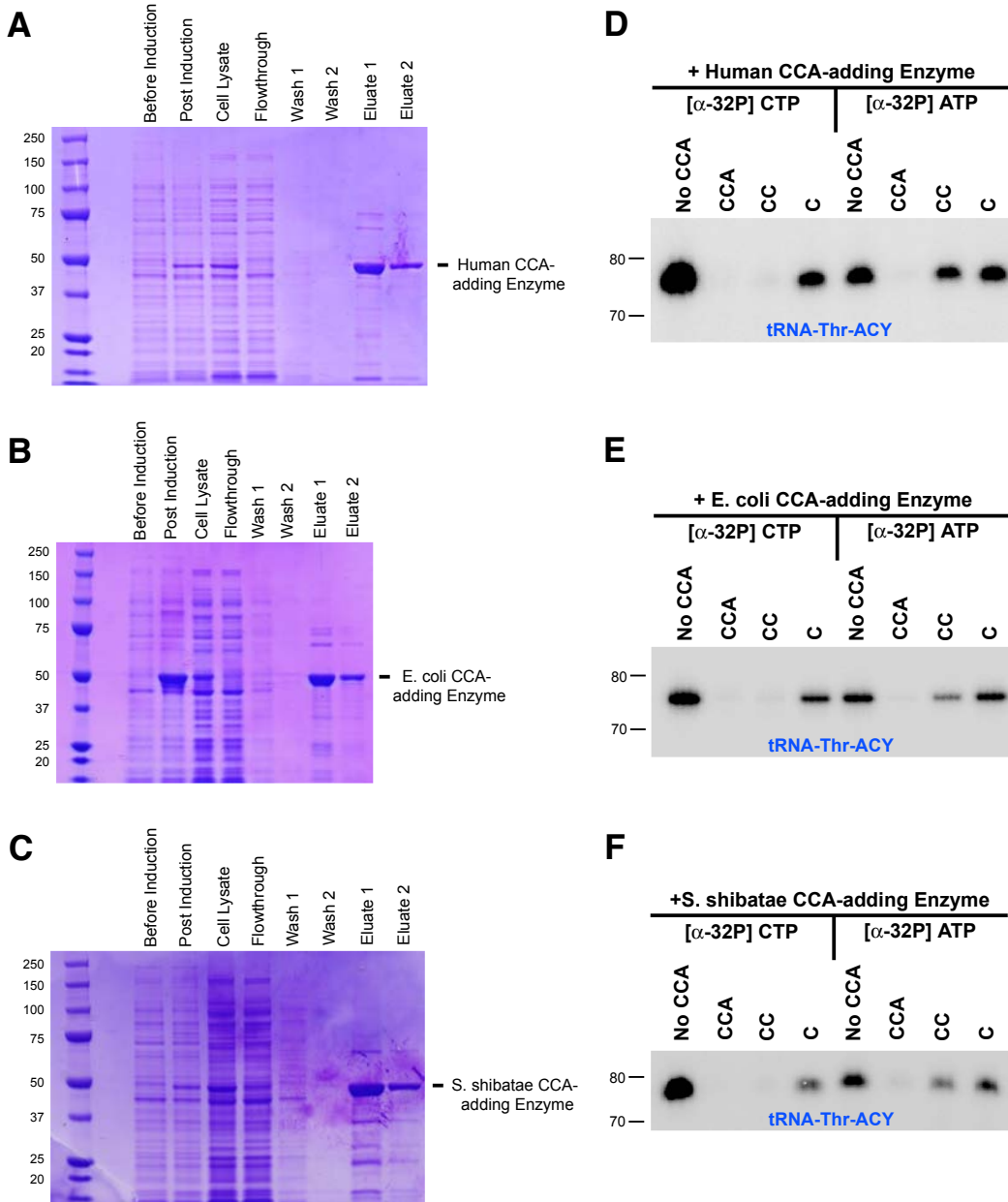


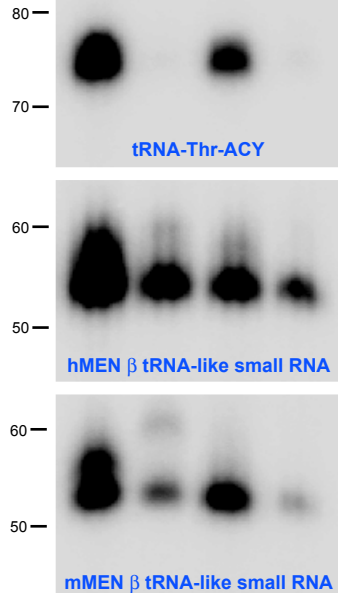
Figure S2

A

+ E. coli CCA-adding Enzyme

[α -32P] CTP [α -32P] ATP

No CCA CCA No CCA CCA

**B**mMEN β Substrate

GCACCTCGGGCCAGGGTTCGAGTCCCTGCAGTACCG

mMEN β 3' RACE 1GCACCTCGGGCCAGGGTTCGAGTCCCTGCAGTACCG **CCACCA**tttaaccgtgaattccagcmMEN β 3' RACE 2GCACCTCGGGCCAGGGTTCGAGTCCCTGCAGTACCG **CCAC**tttaaccgcgaattccagcmMEN β 3' RACE 3GCACCTCGGGCCAGGGTTCGAGTCCCTGCAGTACCG **CCACCA**tttaaccgcgaattccagcmMEN β 3' RACE 4GCACCTCGGGCCAGGGTTCGAGTCCCTGCAGTACCG **CCAC**tttaaccgcgaattccagcmMEN β 3' RACE 5GtACCTCGGGCCAGGGTTCGAGTCCCTGCAGTACCG **CCAC**tttaaccgcgaattccagcmMEN β 3' RACE 6GCACCTCGGGCCAGGGTTCGAGTCCCTGCAGTACCG **CCACCA**tttaaccgcgaattccagcmMEN β 3' RACE 7GCACCTCGGGCCAGGGTTCGAGTCCCTGCAGTACCG **CCACCA**tttaaccgcgaattccagc

Ligated 3' Linker

Figure S3

A

Acceptor Stem D Arm Anticodon Arm T Arm

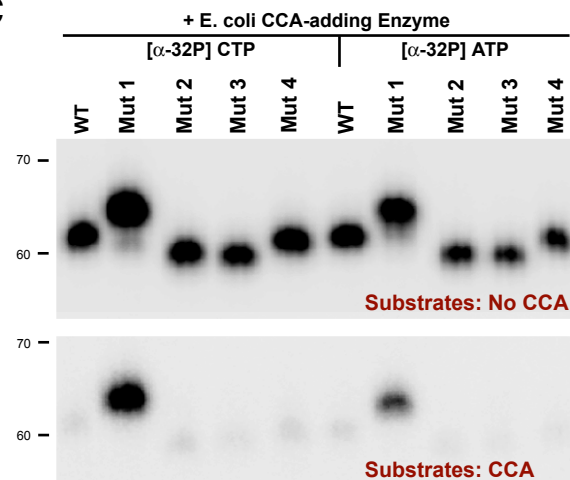
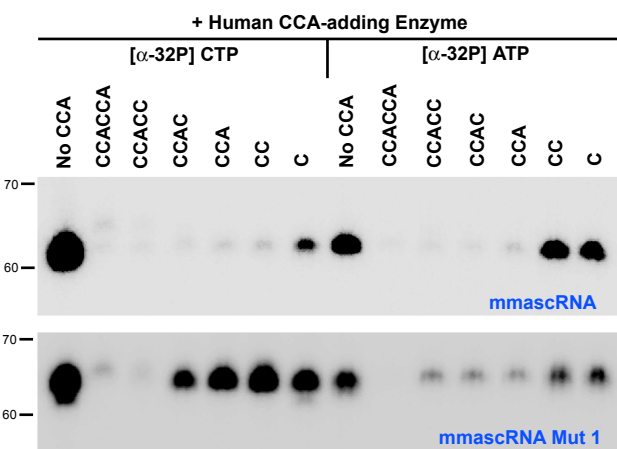
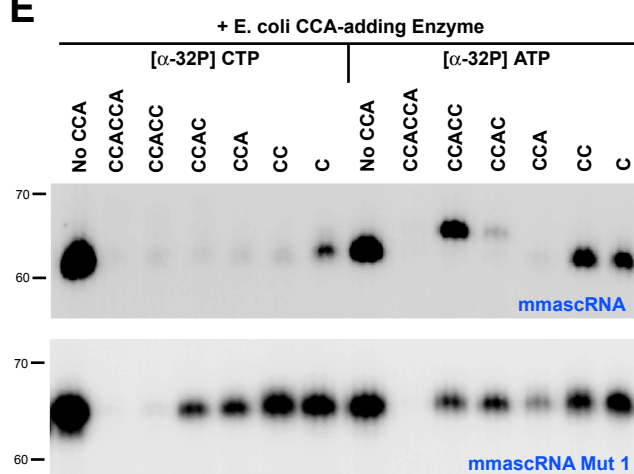
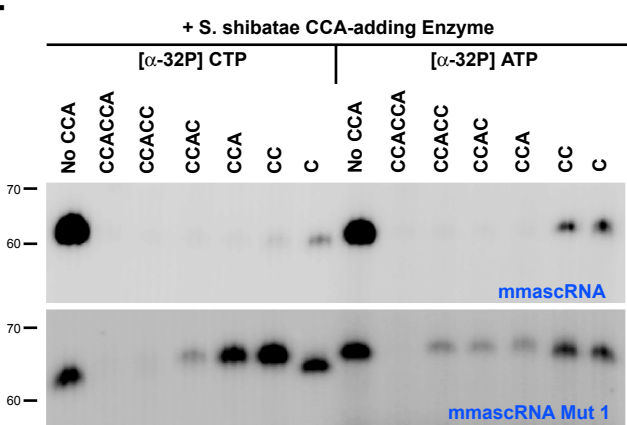
mmasCRNA Mut 1 ggcactgGTGGCTGGCACTCCTGGTTCCAGGACGGGGTTCAAGTCCCTGcagtaccg
 mmasCRNA Mut 2 GACGCTGgtggc*ggcacTCCTGGTTCCAGGACGGGGTTCAAGTCCCTGC CGGTGTCT
 mmasCRNA Mut 3 GACGCTGGTGGCTGGCACgccccacacctcgccgagggttcgagtcctgcagtaccg
 mmasCRNA Mut 4 GACGCTGGTGGCTGGCACTCCTGGTTCCAGGACagggttcgagtcctgc CGGTGTCT

B**mmasCRNA 3' RACE**

3' RACE 1 GACGCTGGTGGCTGGCACTCCTGGTTCCAGGACGGGGTTCAAGTCCCTGC CGGTGTCT CCA ttaaccgcgaattccagc
 Ligated 3' Linker

mmasCRNA Mut 1 3' RACE

3' RACE 1 ggcactgGTGGCTGGCACTCCTGGTTCCAGGACGGGGTTCAAGTCCCTGcagtaccg CCA ttaaccgcgaattccagc
 3' RACE 2 ggcactgGTGGCTGGCACTCCTGGTTCCAGGACGGGGTTCAAGTCCCTGcagtaccg CCA ttaaccgcgaattccagc
 3' RACE 3 ggcactgGTGGCTGGCACTCCTGGTTCCAGGACGGGGTTCAAGTCCCTGcagtaccg CCA ttaaccgcgaattccagc
 3' RACE 4 ggcactgGTGGCTGGCACTCCTGGTTCCAGGACGGGGTTCAAGTCCCTGcagtaccg CCA ttaaccgcgaattccagc
 3' RACE 5 ggcactgGTGGCTGGCACTCCTGGTTCCAGGACGGGGTTCAAGTCCCTGcagtaccg CCA ttaaccgcgaattccagc
 3' RACE 6 ggcactgGTGGCTGGCACTCCTGGTTCCAGGACGGGGTTCAAGTCCCTGcagtaccg CCA ttaaccgcgaattccagc
 3' RACE 7 ggcactgGTGGCTGGCACTCCTGGTTCCAGGACGGGGTTCAAGTCCCTGcagtaccg CCA ttaaccgcgaattccagc
 3' RACE 8 ggcactgGTGGCTGGCACTCCTGGTTCCAGGACGGGGTTCAAGTCCCTGcagtaccg CCA ttaaccgcgaattccagc
 Ligated 3' Linker

C**D****E****F****Figure S4**

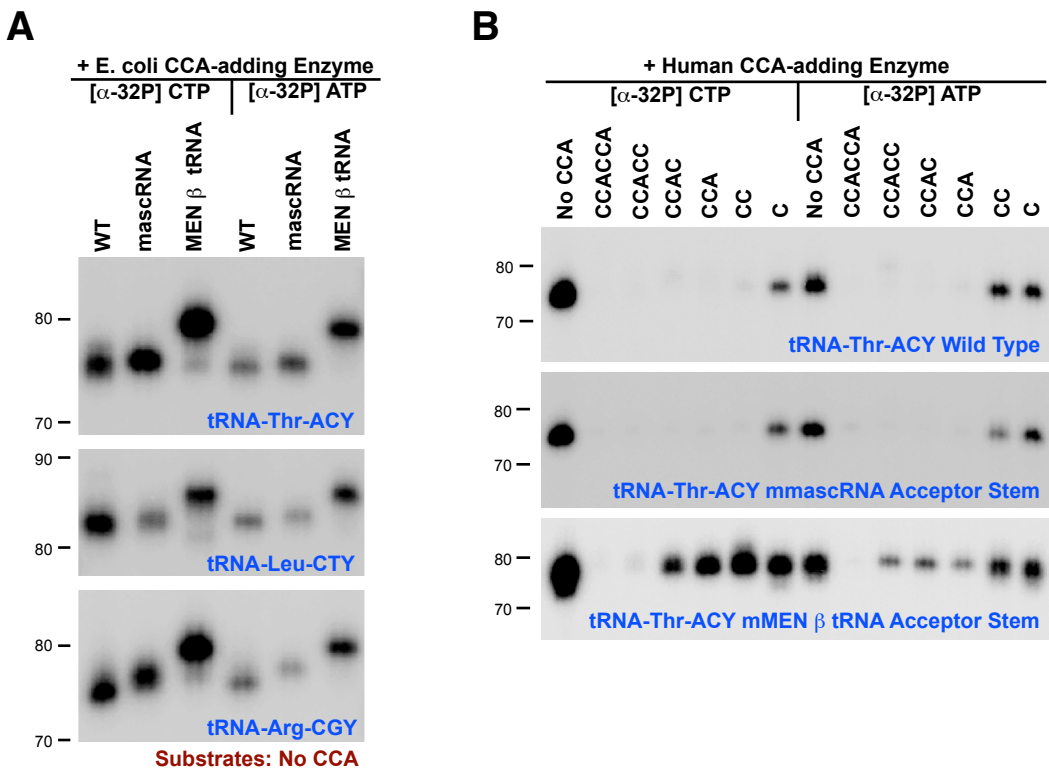


Figure S5

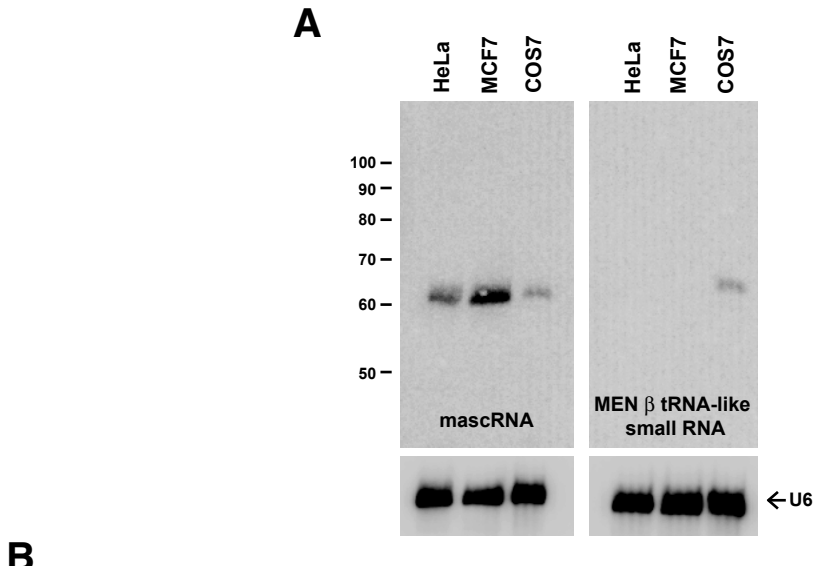
mascRNA

Human	gatgctgggtggcactcctgg-ttt--cc--aggacgggttcaaatccctgcggcgtct
Chimpa.....
Orangutana.....
Rhesusa.....
Baboona.....
Tree shrewc.a.....t.....a.....a.....
Mouse	..c.....c.....g.....t.....
Kangaroo ratc.....t.....g.....c.....t.....
Guinea piga.t.....
Rabbita.....
Pikat.g.....c.....a.....
Alpacaa.....t.....a.....
Cowt.....
Horseg.....
Cata.....
Doga.....a.....t.....a.t.....
Microbatg.g.....t.....
Hedgehoga.ccc....ca.aa.ga.....g.g.....t.....
Elephantt.....a.....
Armadillot.....
Wallaby	...a.....gc.....ta....
Opossum	...a.....-.....c.....a.....g.g.....a.t.....
Platypusg.....a.....a.....a.t.....
X. tropicalis	...a.c.....cc.....t.....t.....
Stickleback	...ct.c.....-.....a.c.ctgt.....tc.....t.....
Medaka	...ct.c.....-.....t....act.....t.....t.....
Zebrafish	...cc.....-a.....a....c.t.....c.....

MEN β tRNA-like small RNA

Human	ggcgctgggtggcacgtccagcacggctggccggggttcgagtccccgcagtgttg
Chimp
Gorillan.....t.....
Orangutant.....
Rhesusa.....ct
Baboona.....t.....ct
Tree shrew	..t.....ac.....t.....a.....ca.cc
Mouse	...a.....c.....c.....c-tc.....a.....t.....accg
Rat	...a.....a.....c...-tg----.....accc
Kangaroo rat	..t.....ca.-a....t.....caccc
Guinea piga.....-a.g.t.....a.....tg.c.ccc
Rabbitc.....c.a-....t.....-.....c.....g.c.ccc
Pikat.....tc.a-....a.....-.....ag.c.ccc
Alpacac.t.....t.....a.....t...tc..cc
Dolphina.....c.tg.t..t.....a.....a.....t.....cc
Cowc.tg....t.....t.....t.....t....c..cc
Horsec.....ac.....t.....a.....tg.c..cc
Dog	.a.....c.....t.....a.....a.....t.tg.c..cc
Hedgehog	c.....tg.....c.tg....t.....g.c..c.
Elephantc..t...gt.....tg.c.cct
Wallaby	...a.....c.....g.c.....-.....tg....ct

Figure S6



B

mascRNA

```

Genome      GTGGTTGGCACTCCTGGTTCCAGGACGGGTTCAAATCCCTGCCGCATTTGCTTG
RACE #1     GTGGTTGGCACTCCTGGTTCCAGGACGGGTTCATATCCCTGCCGCATCTCCAttaaccgcgaattccagctagtc
RACE #2     GTGGTTGGCACTCCTGGTTCCAGGACGGGTTCATATCCCTGCCGCATCTCCAttaaccgcgaattccagctagtc
RACE #3     GTGGTTGGCACTCCTGGTTCCAGGACGGGTTCAGATCCCTGCCGCATCTCCAttaaccgcgaattccagctagtc
RACE #4     GTGGTTGGCACTCCTGGTTCCAGGACGGGTTCATATCCCTGCCGCATCTCCAttaaccgcgaattccagctagtc

```

Ligated 3' Linker

MEN β tRNA-like small RNA

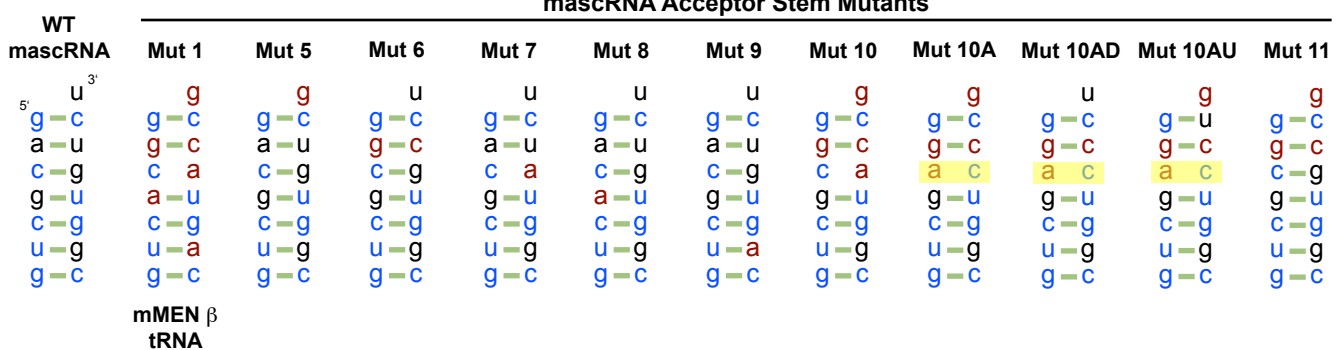
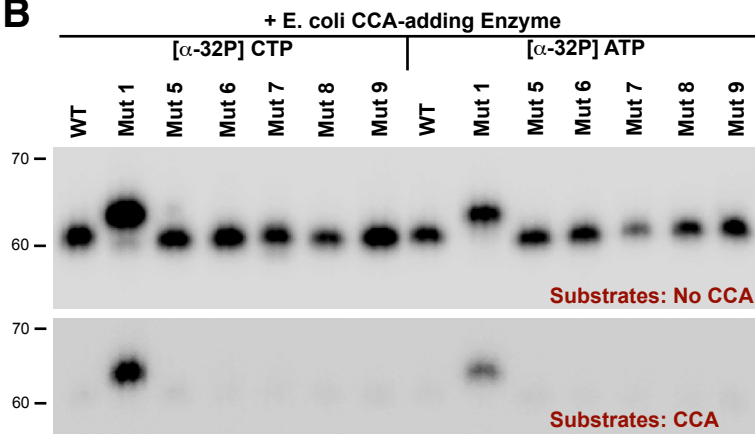
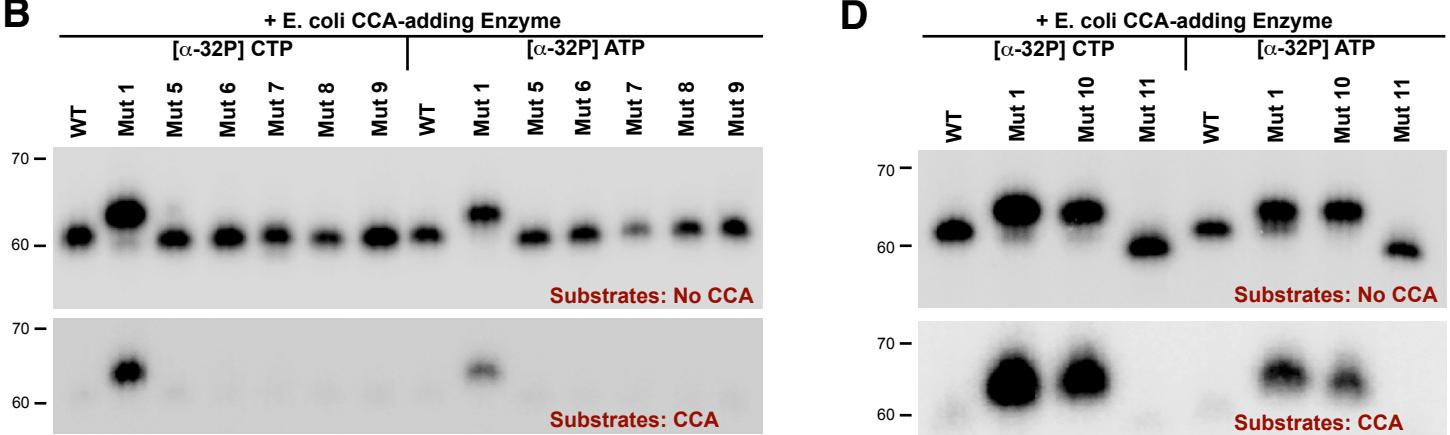
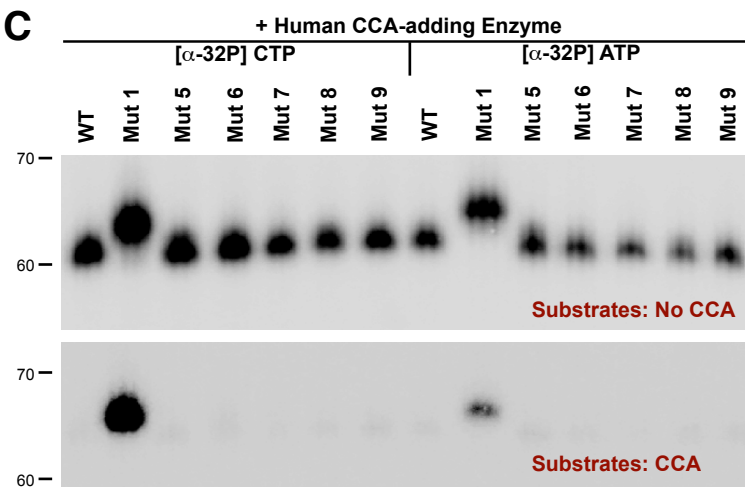
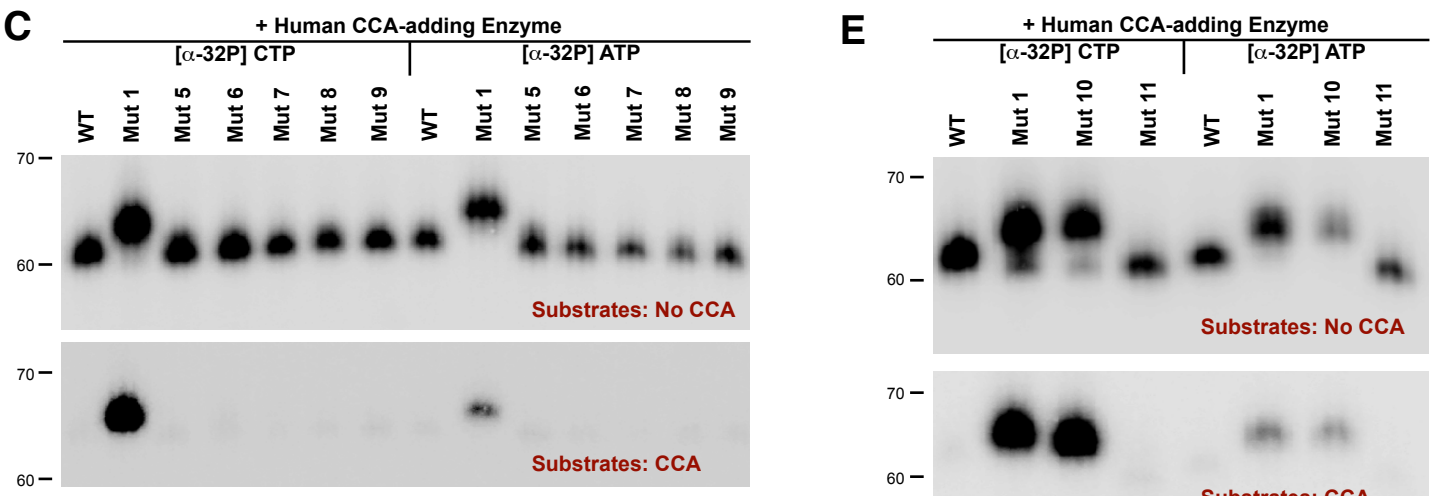
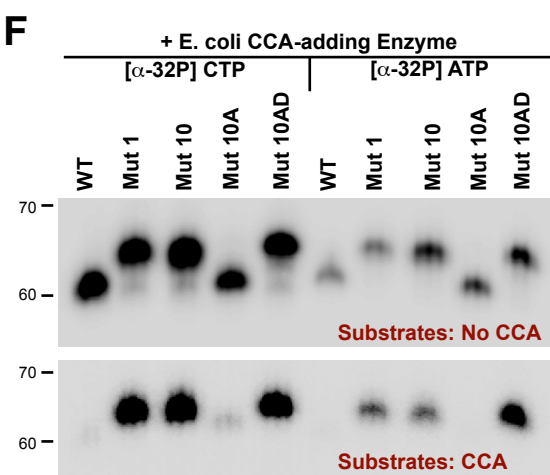
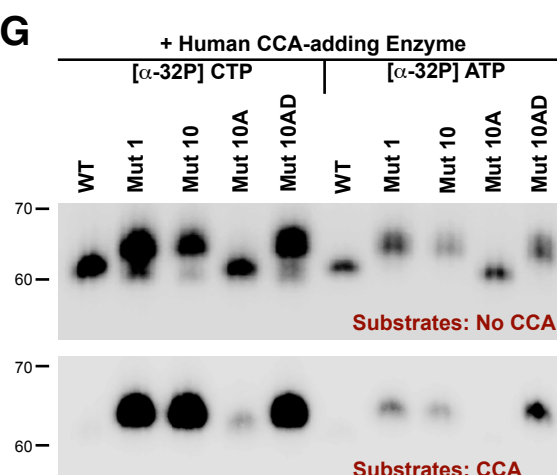
```

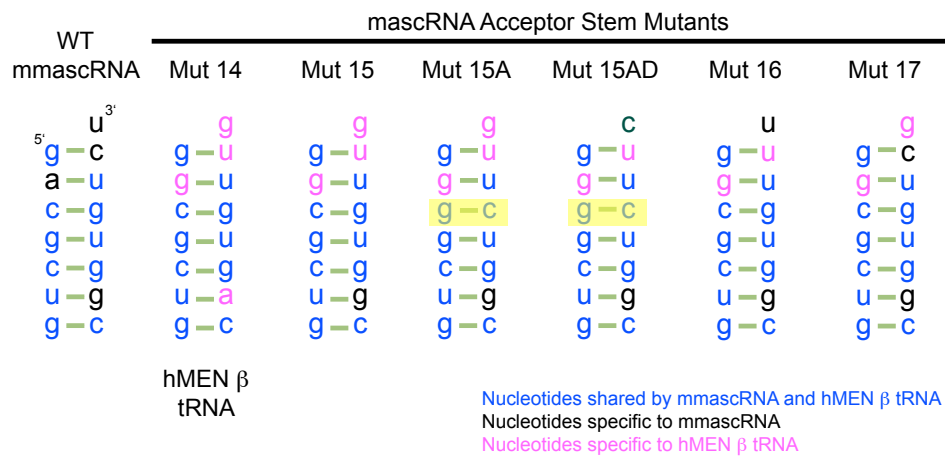
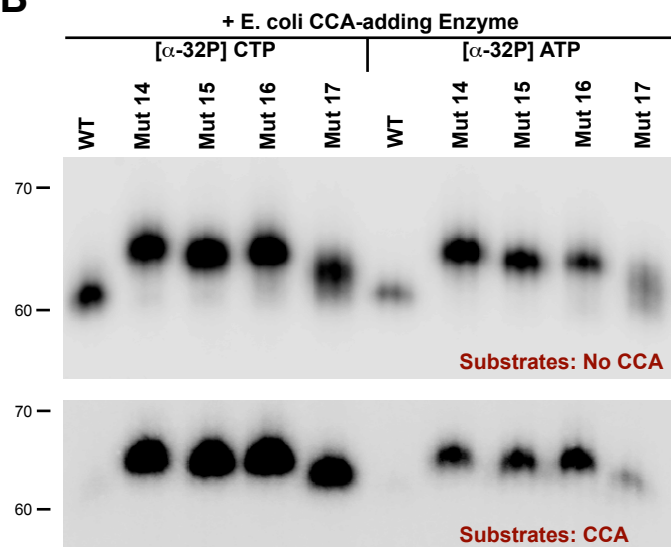
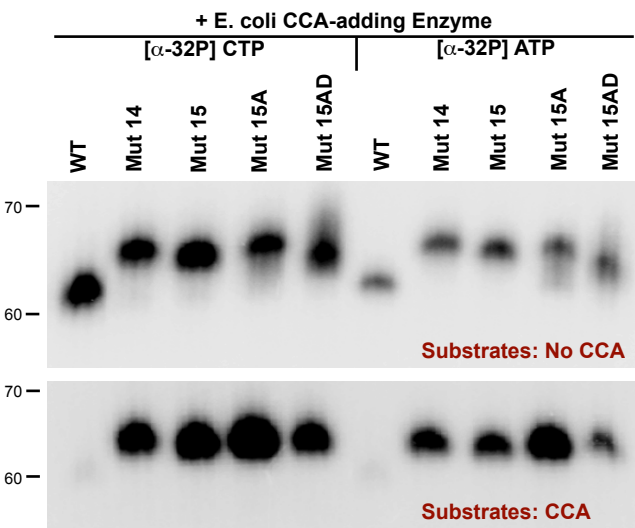
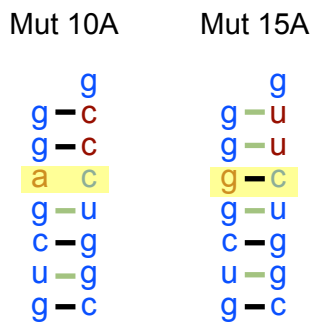
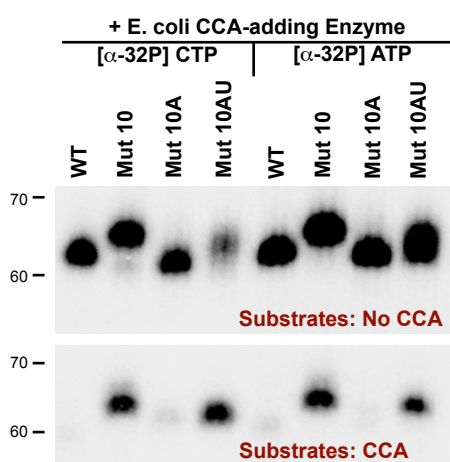
Genome      GTGGTGGCACGTCCAGCACGGCTGGCCGGGTTCGAGTCCCCGCAGTGTCTCTGCTTCC
RACE #1     GTGGTGGCACGTCCAGCACGGCTGGCCGGGTTCGAGTCCCCGCAGTGTCTCCAttaaccgcgaattccagctagtc
RACE #2     GTGGTGGCACGTCCAGCACGGCTGGCCGGGTTCGAGTCCCCGCAGTGTCTCCAttaaccgcgaattccagctagtc
RACE #3     GTGGTGGCACGTCCAGCACGGCTGGCCGGGTTCGAGTCCCCGCAGTGTCTCCAttaaccgcgaattccagctagtc
RACE #4     GTGGTGGCACGTCCAGCACGGCTGGCCGGGTTCGAGTCCCCGCAGTGTCTCCAttaaccgcgaattccagctagtc
RACE #5     GTGGTGGCACGTCCAGCACGGCTGGCCGGGTTCGAGTCCCCGCAGTGTCTCCAttaaccgcgaattccagctagtc
RACE #6     GTGGTGGCACGTCCAGCACGGCTGGCCGGGTTCGAGTCCCCGCAGTGTCTCCAttaaccgcgaattccagctagtc
RACE #7     GTGGTGGCACGTCCAGCACGGCTGGCCGGGTTCGAGTCCCCGCAGTGTCTCCAttaaccgcgaattccagctagtc
RACE #8     GTGGTGGCACGTCCAGCACGGCTGGCCGGGTTCGAGTCCCCGCAGTGTCTCCAttaaccgcgaattccagctagtc
RACE #9     GTGGTGGCACGTCCAGCACGGCTGGCCGGGTTCGAGTCCCCGCAGTGTCTCCAttaaccgcgaattccagctagtc
RACE #10    GTGGTGGCACGTCCAGCACGGCTGGCCGGGTTCGAGTCCCCGCAGTGTCTCCAttaaccgcgaattccagctagtc
RACE #11    GTGGTGGCACGTCCAGCACGGCTGGCCGGGTTCGAGTCCCCGCAGTGTCTCCAttaaccgcgaattccagctagtc

```

Ligated 3' Linker

Figure S7

A**B****D****C****E****F****G****Figure S8**

A**B****C****D****E****Figure S9**

A

WT mMEN β tRNA	mMEN β tRNA Acceptor Stem Mutants						
	Mut 1	Mut 5	Mut 5A	Mut 6	Mut 7	Mut 8	Mut 9
5' g ^{3'}	u	u	u	g	g	g	g
g-c	g-c	g-c	g-c	g-c	g-c	g-c	g-c
g-c	a-u	g-c	g-c	a-u	g-c	g-c	g-c
c-a	c-g	c-a	a-c	c-a	c-g	c-a	c-a
a-u	g-u	a-u	a-u	a-u	a-u	g-u	a-u
c-g	c-g	c-g	c-g	c-g	c-g	c-g	c-g
u-a	u-g	u-a	u-a	u-a	u-a	u-a	u-g
g-c	g-c	g-c	g-c	g-c	g-c	g-c	g-c

mmascRNA

Rule 1: Instability?	Yes	No	Yes	Yes	Yes	No	Yes	Yes
Rule 2: GG at 5' end?	Yes	No	Yes	Yes	No	Yes	Yes	Yes
Rule 3: +3-D base pair? -or- G-U wobble near end?	Yes	No	No	Yes	Yes	Yes	Yes	Yes
Prediction	CCACCA	CCA	CCA	CCACCA	CCA	CCA	CCACCA	CCACCA
Prediction Correct?	Yes	Yes	Yes	Yes	Yes*	Yes	Yes	Yes

Nucleotides shared by mmascRNA and mMEN β tRNA
 Nucleotides specific to mmascRNA
 Nucleotides specific to mMEN β tRNA

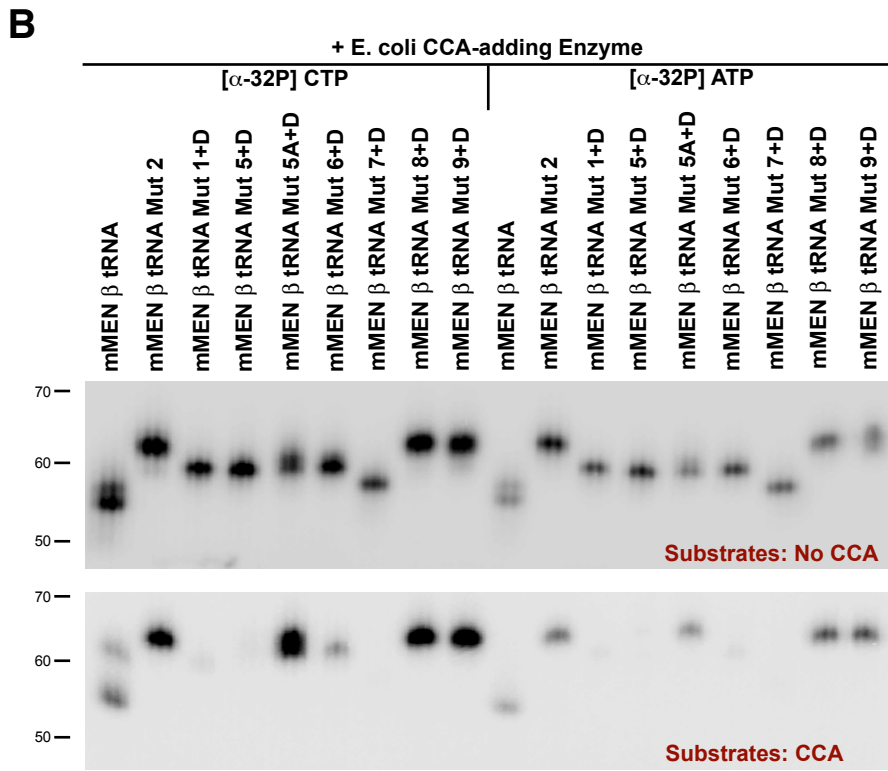


Figure S10

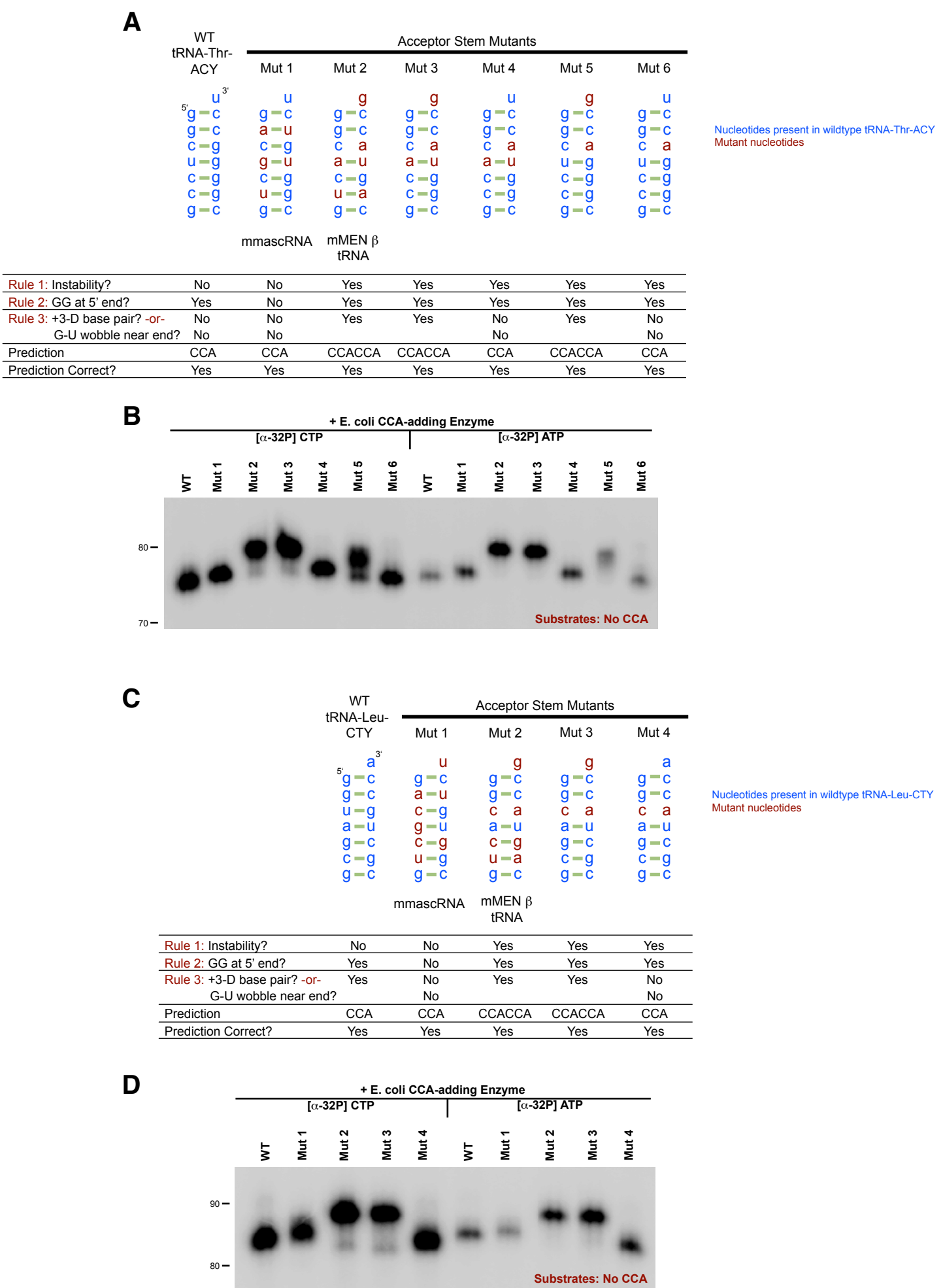


Figure S11

Eukaryotes

	<i>A. thaliana</i>		<i>C. elegans</i>		<i>D. melanogaster</i>		<i>H. sapiens</i>		<i>M. musculus</i>		<i>S. cerevisiae</i>		<i>Z. mays</i>	
	#	%	#	%	#	%	#	%	#	%	#	%	#	%
AA	2	0.3	2	0.2	0	0.0	1	0.2	0	0.0	1	0.3	0	0.0
AC	1	0.2	7	0.9	0	0.0	12	1.9	8	1.8	0	0.0	70	6.0
AG	7	1.1	13	1.6	6	2.0	13	2.1	11	2.5	6	2.0	31	2.7
AU	9	1.4	1	0.1	0	0.0	2	0.3	0	0.0	2	0.7	20	1.7
CA	2	0.3	3	0.4	0	0.0	1	0.2	0	0.0	0	0.0	1	0.1
CC	70	11.0	20	2.4	9	3.0	21	3.3	10	2.3	0	0.0	15	1.3
CG	1	0.2	6	0.7	0	0.0	1	0.2	0	0.0	0	0.0	3	0.3
CU	2	0.3	2	0.2	1	0.3	4	0.6	1	0.2	8	2.7	0	0.0
GA	30	4.7	48	5.9	26	8.6	28	4.4	21	4.8	19	6.4	64	5.5
GC	152	23.8	346	42.2	103	33.9	128	20.3	93	21.5	92	31.2	330	28.3
GG	203	31.8	241	29.4	92	30.3	238	37.7	189	43.6	109	36.9	411	35.2
GU	130	20.3	39	4.8	28	9.2	105	16.6	60	13.9	11	3.7	149	12.8
UA	1	0.2	2	0.2	0	0.0	16	2.5	0	0.0	0	0.0	0	0.0
UC	27	4.2	80	9.8	39	12.8	50	7.9	38	8.8	39	13.2	67	5.7
UG	2	0.3	9	1.1	0	0.0	6	1.0	2	0.5	2	0.7	6	0.5
UU	0	0.0	1	0.1	0	0.0	5	0.8	0	0.0	6	2.0	1	0.1
Total	639		820		304		631		433		295		1168	

Summary

	All 16 Species	
	#	%
AA	6	0.1
AC	102	2.1
AG	115	2.4
AU	34	0.7
CA	7	0.1
CC	151	3.1
CG	39	0.8
CU	19	0.4
GA	238	4.9
GC	1448	30.1
GG	1687	35.1
GU	545	11.3
UA	20	0.4
UC	352	7.3
UG	36	0.7
UU	13	0.3
Total	4812	

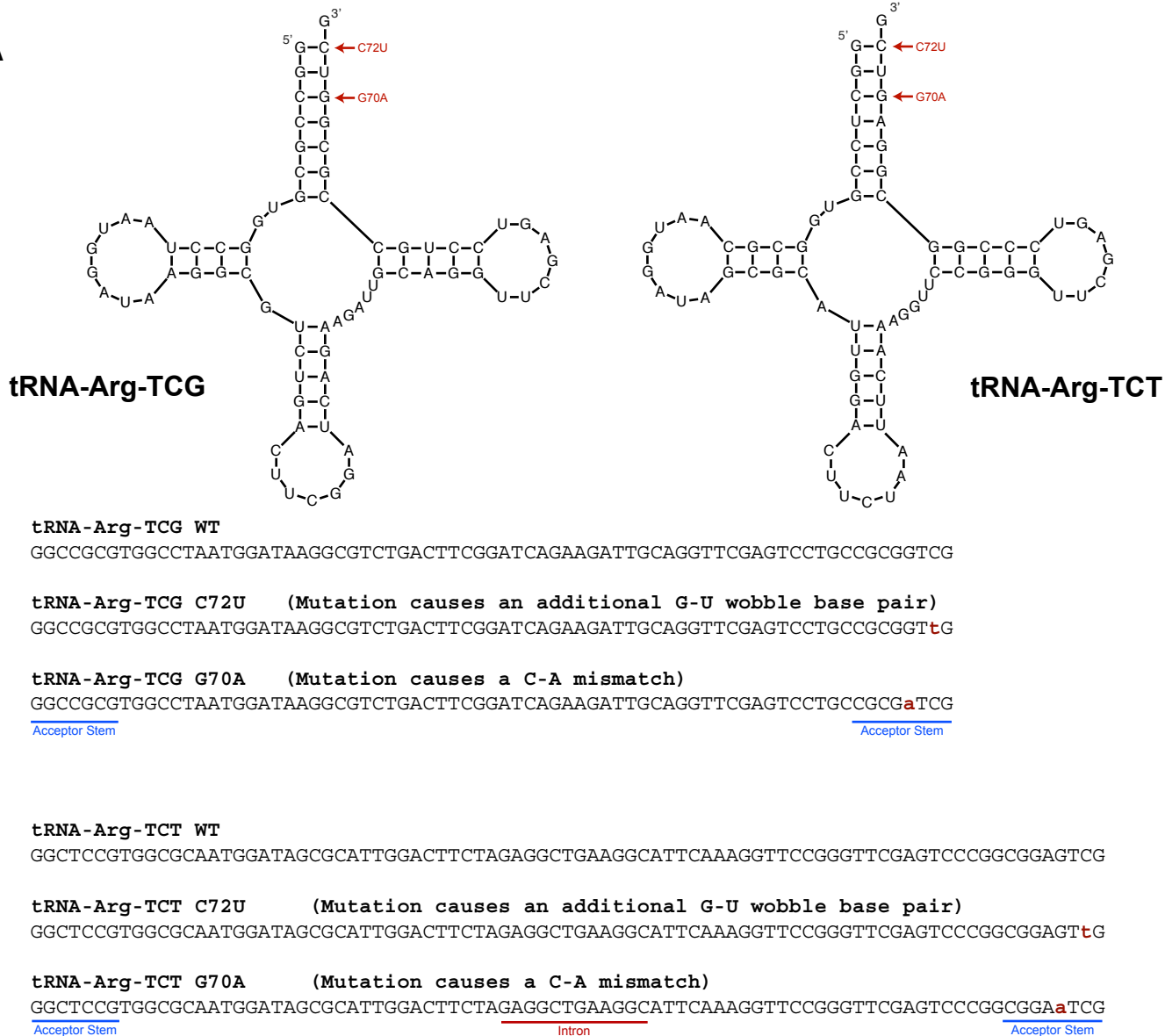
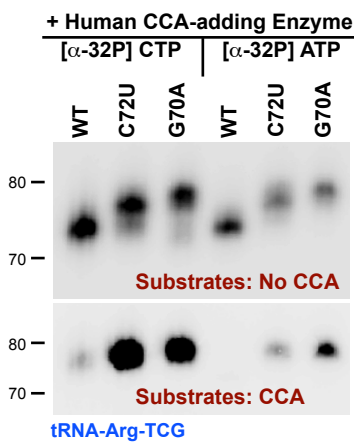
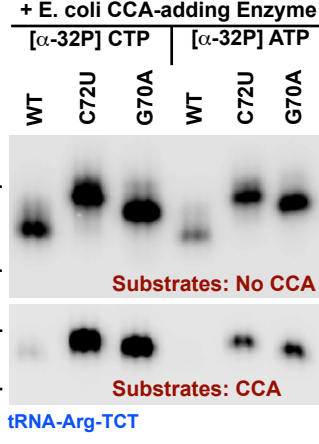
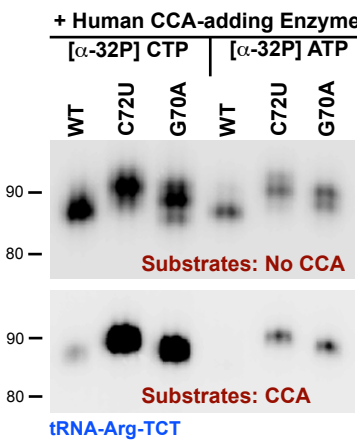
Eubacteria

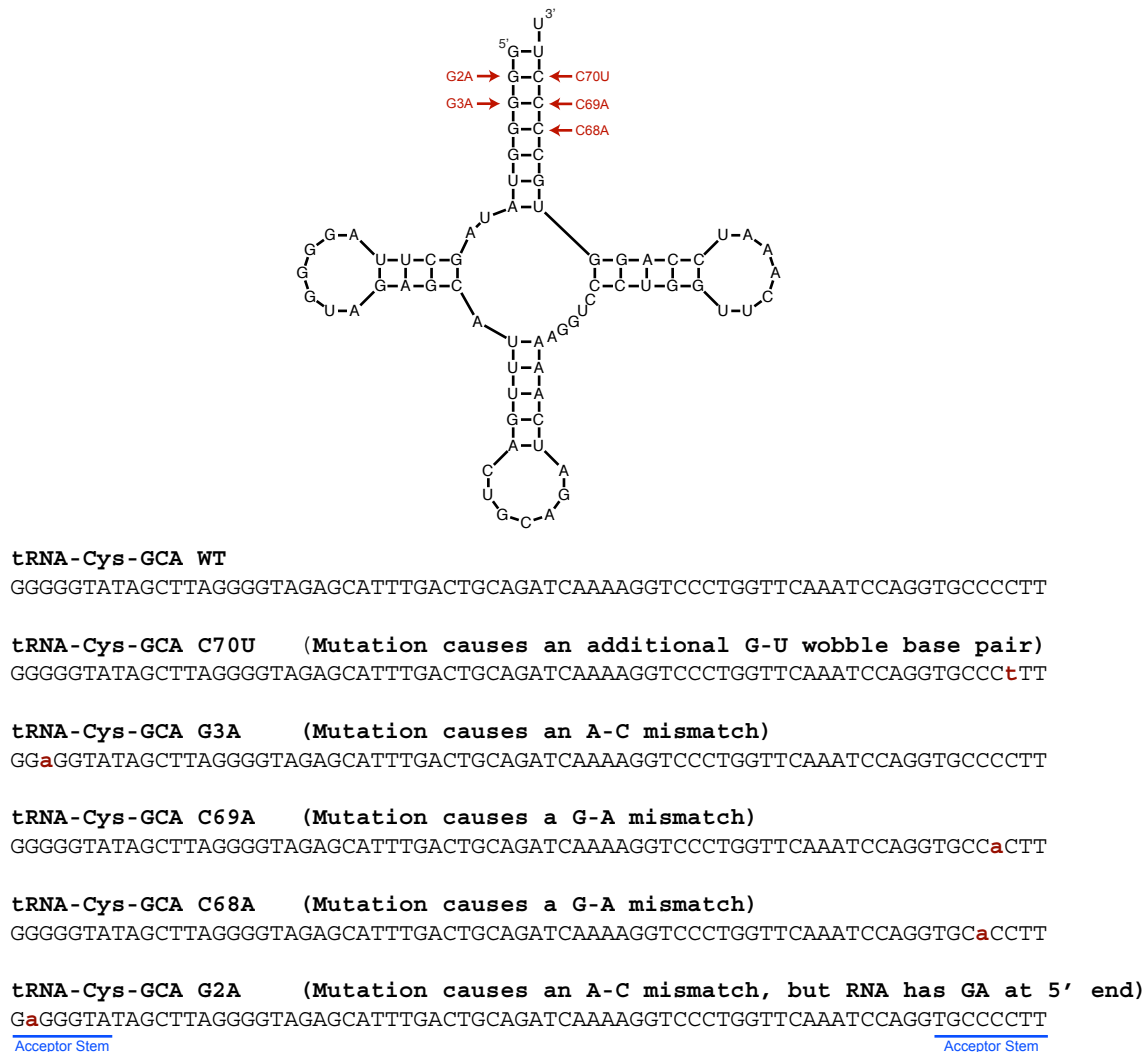
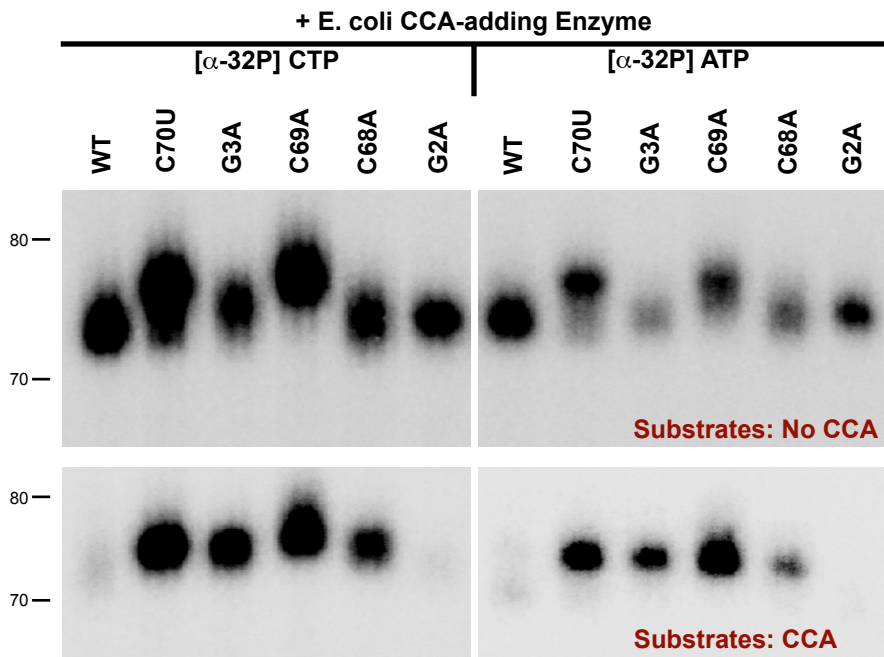
	<i>E. coli K12</i>		<i>H. influenzae</i>		<i>M. tuberculosis</i>		<i>M. pneumoniae</i>		<i>V. cholerae</i>	
	#	%	#	%	#	%	#	%	#	%
AA	0	0.0	0	0.0	0	0.0	0	0.0	0	0.0
AC	0	0.0	0	0.0	0	0.0	0	0.0	0	0.0
AG	4	4.5	1	1.7	1	2.2	1	2.7	6	6.1
AU	0	0.0	0	0.0	0	0.0	0	0.0	0	0.0
CA	0	0.0	0	0.0	0	0.0	0	0.0	0	0.0
CC	1	1.1	1	1.7	0	0.0	1	2.7	0	0.0
CG	7	8.0	4	6.9	4	8.9	2	5.4	9	9.2
CU	0	0.0	0	0.0	0	0.0	1	2.7	0	0.0
GA	0	0.0	0	0.0	0	0.0	1	2.7	0	0.0
GC	29	33.0	17	29.3	17	37.8	11	29.7	39	39.8
GG	33	37.5	26	44.8	18	40.0	16	43.2	34	34.7
GU	6	6.8	4	6.9	2	4.4	2	5.4	6	6.1
UA	0	0.0	0	0.0	0	0.0	1	2.7	0	0.0
UC	4	4.5	2	3.4	2	4.4	0	0.0	4	4.1
UG	4	4.5	3	5.2	1	2.2	1	2.7	0	0.0
UU	0	0.0	0	0.0	0	0.0	0	0.0	0	0.0
Total	88		58		45		37		98	

Archaea

	<i>K. cryptofilum</i>		<i>M. acetivorans</i>		<i>N. equitans</i>		<i>S. solfataricus</i>	
	#	%	#	%	#	%	#	%
AA	0	0.0	0	0.0	0	0.0	0	0.0
AC	0	0.0	4	6.7	0	0.0	0	0.0
AG	3	6.5	7	11.7	2	4.5	3	6.5
AU	0	0.0	0	0.0	0	0.0	0	0.0
CA	0	0.0	0	0.0	0	0.0	0	0.0
CC	0	0.0	1	1.7	1	2.3	1	2.2
CG	1	2.2	0	0.0	1	2.3	0	0.0
CU	0	0.0	0	0.0	0	0.0	0	0.0
GA	0	0.0	1	1.7	0	0.0	0	0.0
GC	22	47.8	25	41.7	21	47.7	23	50.0
GG	20	43.5	19	31.7	19	43.2	19	41.3
GU	0	0.0	3	5.0	0	0.0	0	0.0
UA	0	0.0	0	0.0	0	0.0	0	0.0
UC	0	0.0	0	0.0	0	0.0	0	0.0
UG	0	0.0	0	0.0	0	0.0	0	0.0
UU	0	0.0	0	0.0	0	0.0	0	0.0
Total	46		60		44		46	

Figure S12

A**B****C****Figure S13**

A**B****Figure S14**

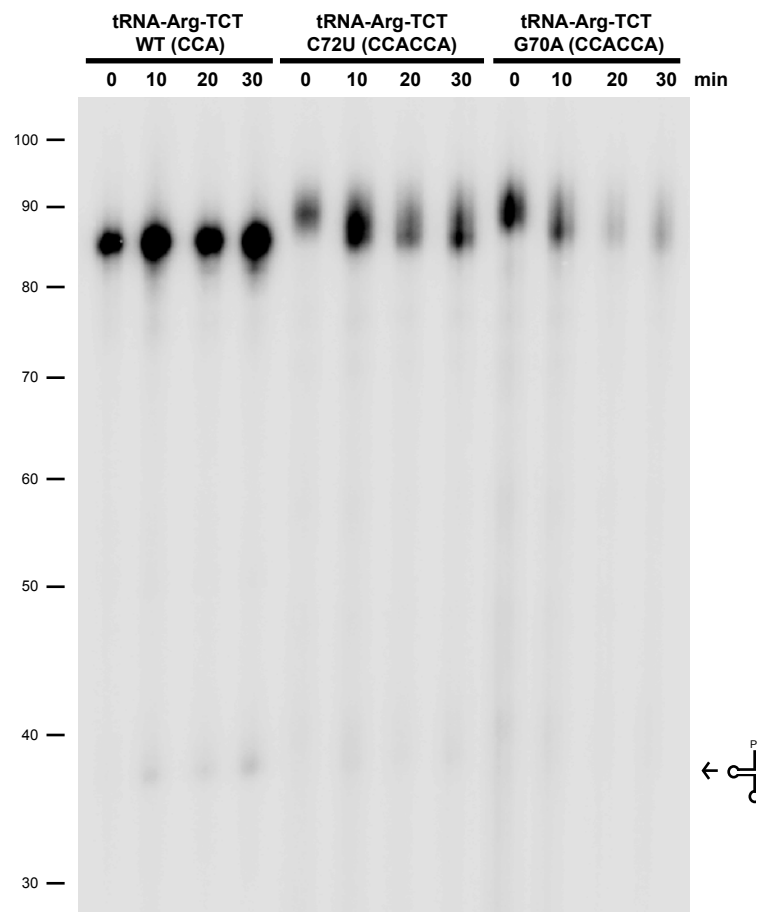
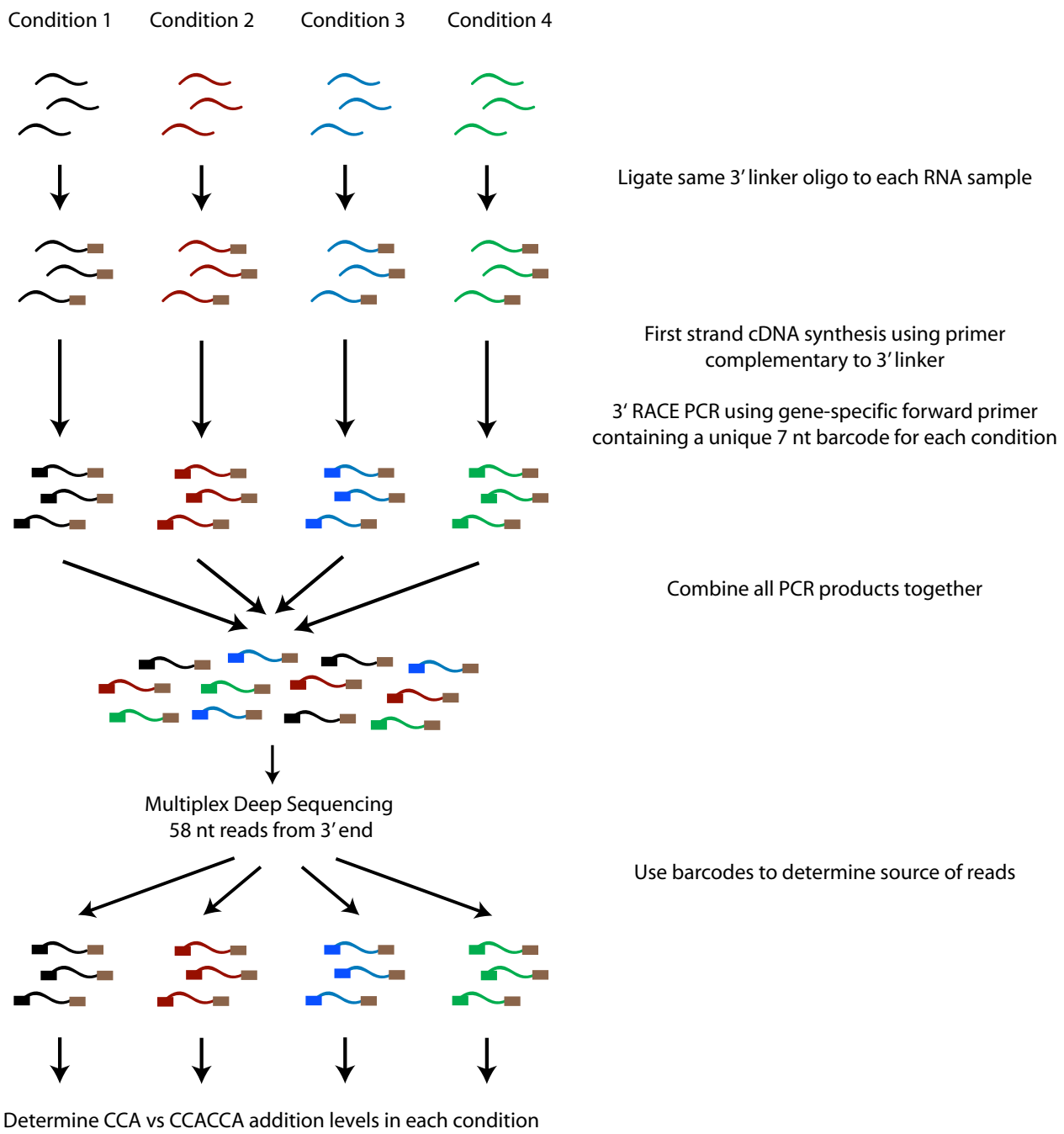
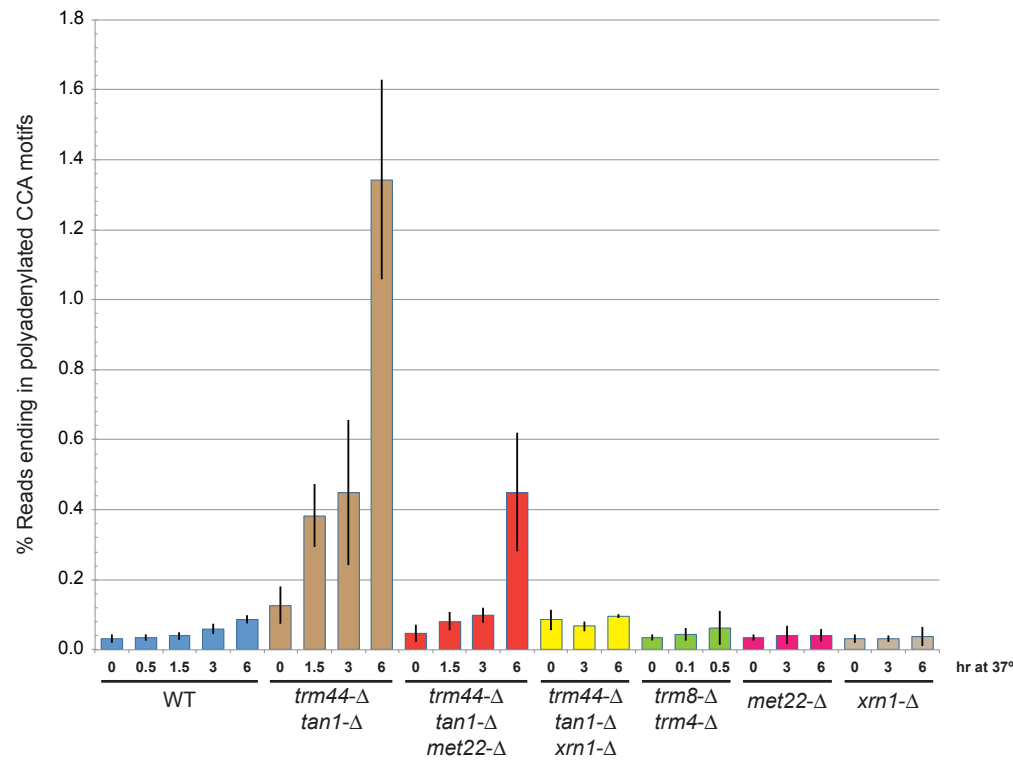
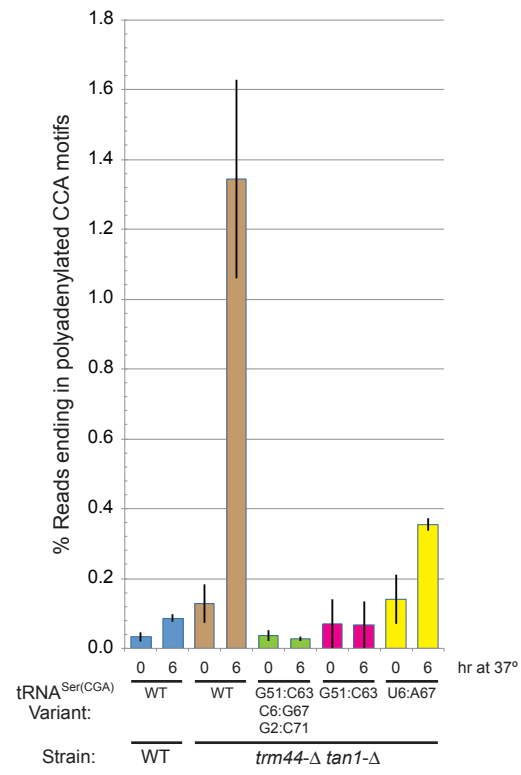


Figure S15

A**B****Figure S16**

A**B****Figure S17**

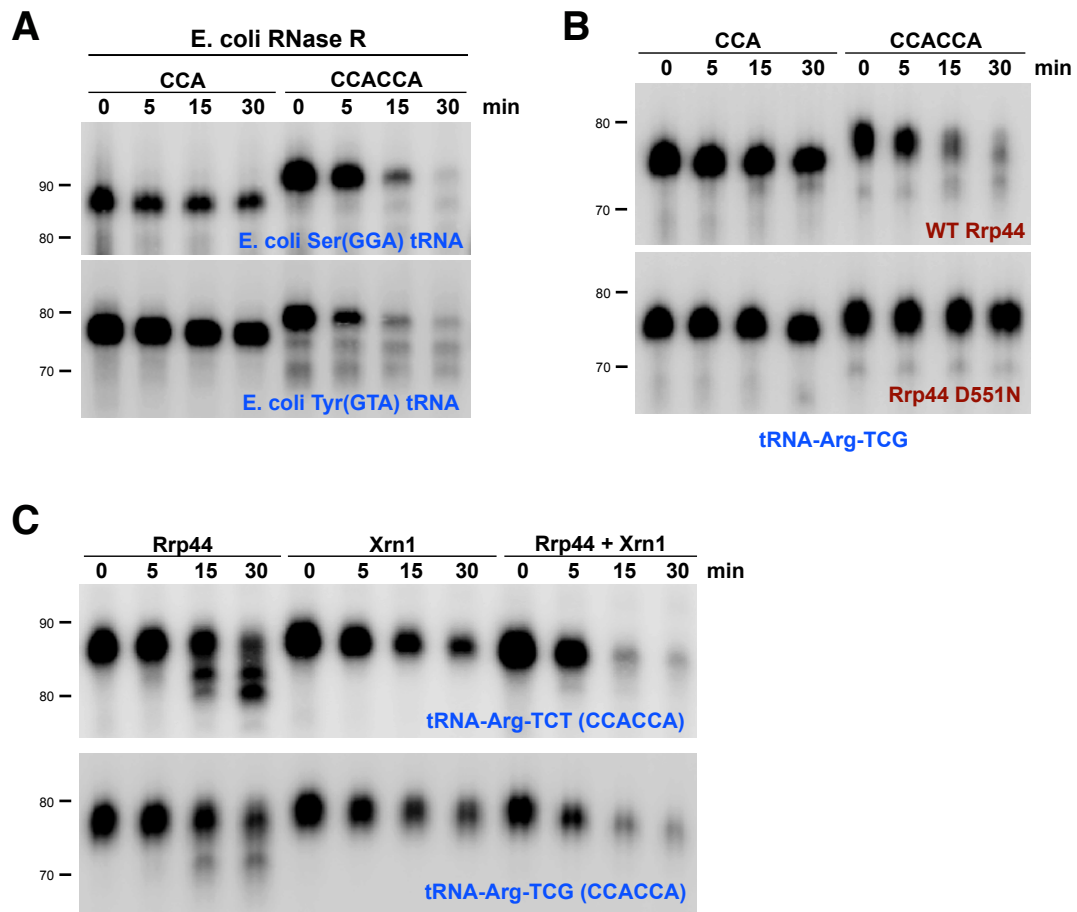


Figure S18

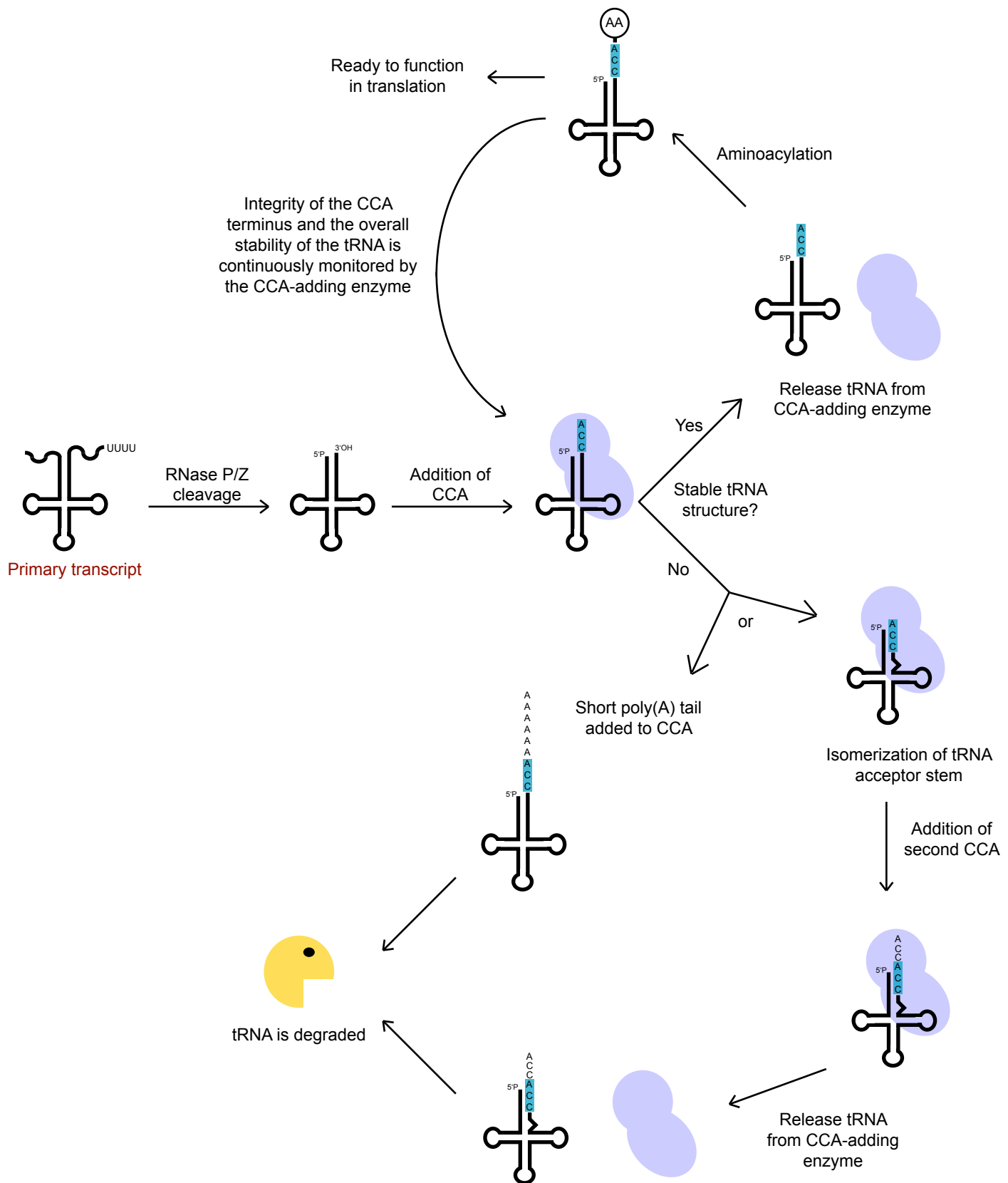
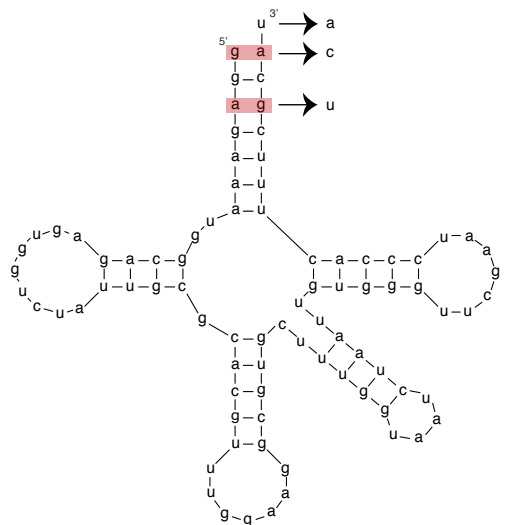
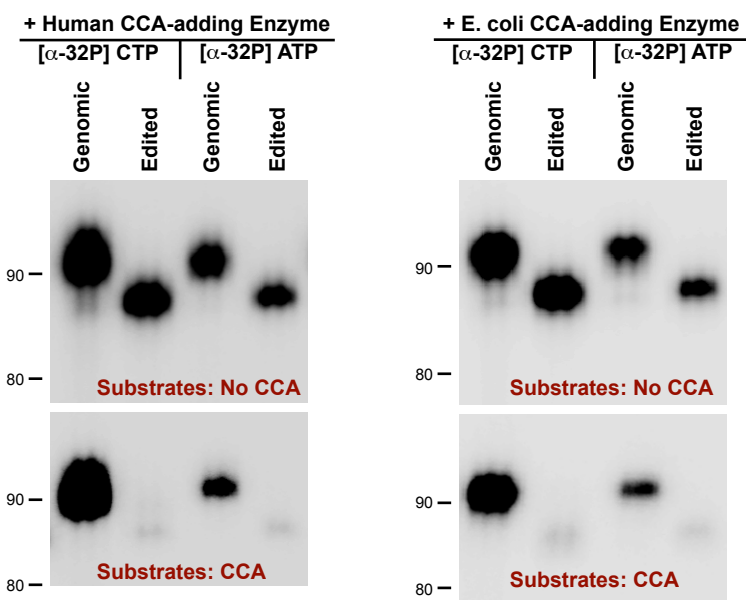
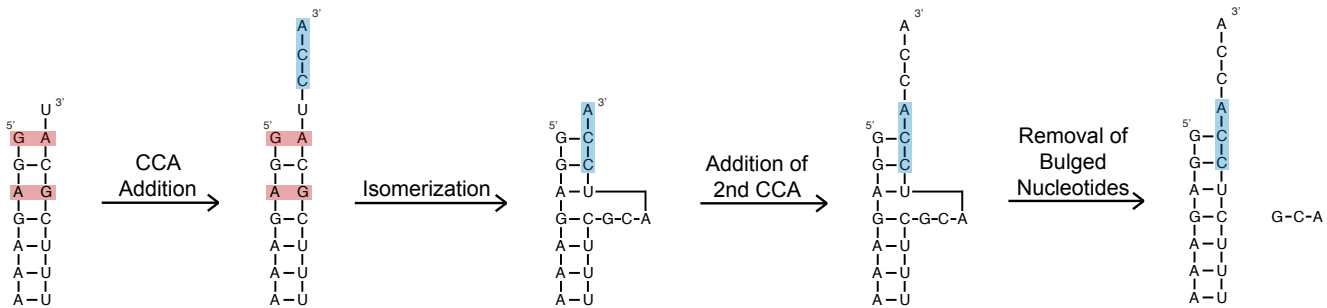


Figure S19

A

Seculamonas ecuadorensis
mitochondrial tRNA^{Ser}

**B****C****D**

Acanthamoeba castellanii
mitochondrial tRNA^{Ala}

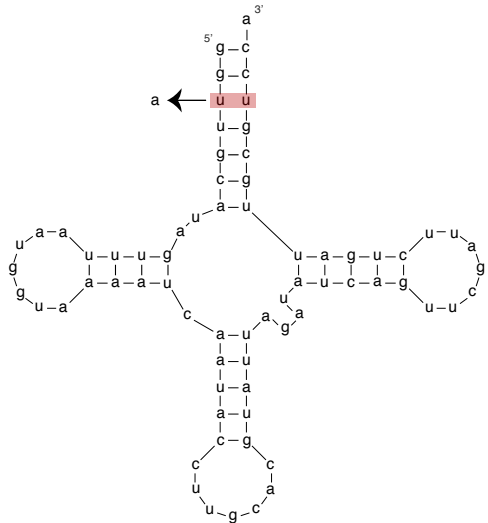
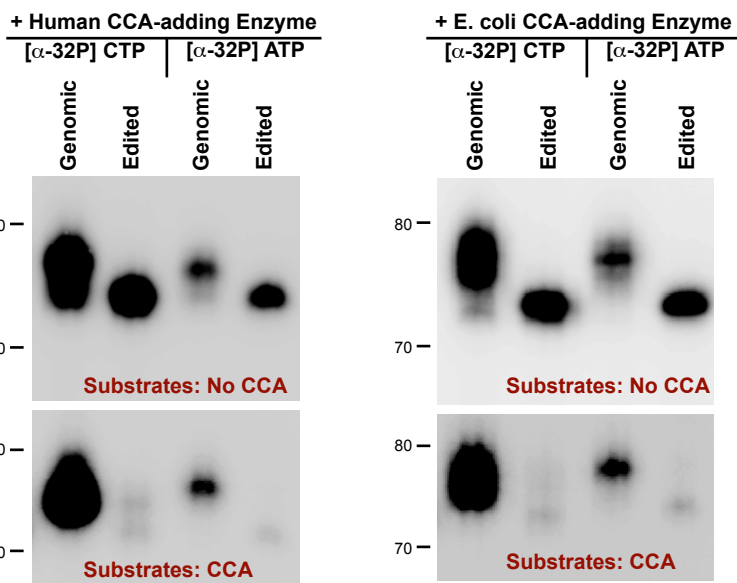
**E****Figure S20**

Table S1

Strain	Time at 37	Replicate #	Total Reads	CCA	CCAC	CCACC	CCACCA	CCACCCAC	CCA x3	SUM	% Extended CCA Motifs	Average	Stdev	Relative Level	Stdev
WT (JMW007)	0 hr	1	2,383,825	1,720,410	14	8	6	2		28	0.00163	0.00371	0.00261	1.00	0.70
		2	2,836,577	2,215,590	27	2	3			32	0.00144				
		3	2,119,015	1,643,012	96	2	13			111	0.00676				
		4	2,147,056	1,740,053	67	4	16			87	0.00500				
WT (JMW007)	0.5 hr	1	3,131,139	2,387,937	36	8	6			50	0.00209	0.00283	0.00058	0.76	0.16
		2	2,080,275	1,741,691	37	4	5			46	0.00264				
		3	1,863,204	1,561,183	38	5	7			50	0.00320				
		4	2,382,333	1,954,507	55	3	8			66	0.00338				
WT (JMW007)	1.5 hr	1	1,763,183	1,457,321	30	8	4			42	0.00288	0.00323	0.00136	0.87	0.37
		2	1,807,474	1,480,671	55	8	7			70	0.00473				
		3	2,450,329	1,985,101	26	7	8			41	0.00207				
		4	2,238,661	1,788,351	34	13	5			52	0.00291				
WT (JMW007)	3 hr	1	3,363,888	2,619,879	50	9	7	2		66	0.00252	0.00273	0.00037	0.73	0.10
		2	1,774,037	1,456,810	24	8	2			34	0.00233				
		3	1,940,037	1,558,880	30	15	4			49	0.00314				
		4	2,238,661	1,788,351	34	13	5			52	0.00291				
WT (JMW007)	6 hr	1	2,145,677	1,511,288	59	41	11			111	0.00734	0.01224	0.00527	3.30	1.42
		2	2,431,609	1,610,373	180	80	27	3		287	0.01782				
		3	2,522,427	1,790,013	141	51	15	4	4	207	0.01156				
		4	2,533,264	1,713,750	101	26	10	2		137	0.00799	0.00782	0.00381	2.11	1.03
trm44-Δ tan1-Δ (JMW119)	0 hr	1	1,847,577	1,292,496	26	6	8			40	0.00309				
		2	1,954,117	1,405,172	48	2	8			58	0.00413				
		3	2,028,146	1,377,183	87	14	6	3	2	107	0.00777				
		4	1,724,791	1,118,440	62	16	9			87	0.00778				
		5	2,279,391	1,451,951	101	26	6			2	133	0.00916			
		6	1,453,475	808,359	95	13	7			2	3	120	0.01484		
		7	1,425,638	1,078,057	259	90	6			355	0.03293	0.02942	0.00655	7.93	1.76
trm44-Δ tan1-Δ (JMW119)	1.5 hr	1	1,548,559	1,156,582	271	109	7			387	0.03346				
		2	1,786,720	1,413,013	210	89	10			309	0.02187				
		3	1,734,848	1,057,832	400	281	21			702	0.06536	0.04039	0.01349	10.89	3.64
		4	2,421,152	1,830,979	577	262	19			858	0.04686				
		5	2,287,242	1,722,862	424	228	22			674	0.03890				
		6	2,731,860	2,208,457	342	229	24			595	0.02694				
		7	2,606,893	1,995,353	419	215	19			653	0.03273				
trm44-Δ tan1-Δ (JMW119)	3 hr	1	1,996,874	1,273,668	1,181	1,868	75			3,124	0.24528	0.17440	0.03900	47.01	10.51
		2	2,507,487	1,630,090	1,142	1,492	77	2		2,711	0.16631				
		3	2,558,513	1,754,856	1,074	1,493	69			2,636	0.15021				
		4	1,508,822	1,004,566	585	692	41			1,318	0.13120				
		5	2,026,332	983,072	739	893	53			1,685	0.17140				
		6	1,332,707	657,766	540	598	57	2		1,197	0.18198				
		7	2,376,861	1,420,369	127	7	25			2	161	0.01134			
trm44-Δ tan1-Δ met22-Δ (LY1729)	0 hr	1	3,146,254	2,196,850	62	16	6			84	0.00982	0.00594	0.00388	1.60	1.05
		2	3,635,133	2,813,591	36	3	12	3		51	0.00181				
		3	3,230,696	2,407,540	81	9	21	5	2	111	0.00461				
		4	2,465,954	2,085,947	27	8	10			40	0.00192				
		5	2,010,837	1,391,668	131		11			142	0.01020				
		6	2,603,550	1,422,885	87	7	18	3		112	0.00787				
		7	2,411,522	1,634,700	113	81	7			201	0.01230				
trm44-Δ tan1-Δ met22-Δ (LY1729)	6 hr	1	2,169,513	1,333,937	217	278	23	2		518	0.03883	0.07434	0.02617	20.04	7.05
		2	2,242,083	1,450,098	766	785	29	2		1,580	0.10896				
		3	2,479,794	1,664,930	828	841	20	3	3	1,689	0.10145				
		4	2,380,334	1,655,163	713	328	51			3	1,092	0.06598			
		5	2,371,125	1,609,933	649	372	33				1,054	0.06547			
		6	1,835,683	1,159,536	362	371	5				758	0.06537			
		7	2,547,502	1,733,200	134	17	15				166	0.00958	0.01018	0.00245	2.74
trm44-Δ tan1-Δ met22-Δ (LY1729)	3 hr	1	2,046,207	1,597,518	196	78	12	3	3	286	0.01791				
		2	1,973,749	1,509,434	153	73	18			244	0.01616				
		3	2,334,696	1,831,187	146	62	19			227	0.0240				
		4	2,457,994	1,944,618	226	23	24			273	0.01404				
		5	2,394,726	1,761,193	202	39	31			272	0.01544				
		6	2,376,861	1,420,369	127	7	25			201	0.01230				
		7	2,275,984	1,333,937	217	278	23	2		518	0.03883	0.07434	0.02617	20.04	7.05
trm44-Δ tan1-Δ met22-Δ (LY1729)	0 hr	1	2,169,513	1,333,937	217	278	23	2		518	0.03883	0.07434	0.02617	20.04	7.05
		2	2,242,083	1,450,098	766	785	29	2		1,580	0.10896				
		3	2,479,794	1,664,930	828	841	20	3	3	1,689	0.10145				
		4	2,380,334	1,655,163	713	328	51			3	1,092	0.06598			
		5	2,371,125	1,609,933	649	372	33				1,054	0.06547			
		6	1,835,683	1,159,536	362	371	5				758	0.06537			
		7	2,547,502	1,733,200	134	17	15				166	0.00958	0.01018	0.00245	2.74
trm8-Δ trm4-Δ (JMW009)	0 min	1	3,217,937	2,427,387	44	6	14	2	2	64	0.00264	0.00295	0.00042	0.79	0.11
		2	2,057,657	1,608,303	45	4	3			52	0.00308				
		3	2,243,094	1,781,395	45	3	14			62	0.00348				
		4	2,448,193	2,044,144	42	4	7			53	0.00259				
		5	1,421,347	1,140,327	28	2	4			34	0.00298	0.00256	0.00075	0.69	0.20
		6	1,736,254	1,466,406	35	7	5			47	0.00321				
		7	2,042,023	1,668,629	36	6		2	2	42	0.00252				
trm8-Δ trm4-Δ (JMW009)	30 min	1	3,119,846	2,393,799	53	21	14			88	0.00368	0.00298	0.00070	0.80	0.19
		2	1,724,412	1,436,222	45	5				50	0.00348				
		3	2,117,406	1,775,957	26	8	6			40	0.00225				
		4	1,716,700	1,432,627	27	5	4			36	0.00251				
		5	2,014,730	1,385,676	126					145	0.01046	0.00865	0.00163	2.33	0.44
		6	1,986,129	1,258,600	81	2	20			103	0.00818				
		7	1,342,082	890,977	40	4	13	3	5	65	0.00730				

Table S2

Strain	Time at 37	Replicate #	Total Reads	CCA	CCAC	CCACC	CCACCA	CCACCCAC	CCA x3	SUM	% Extended CCA Motifs	Average	Stdev	Relative Level	Stdev
WT (JMW007)	0 hr	1	2,383,825	1,720,410	14	8	6		2	28	0.00163	0.00371	0.00261	1.00	0.70
		2	2,836,577	2,215,590	27	2	3			32	0.00144				
		3	2,119,015	1,643,012	96	2	13			111	0.00676				
		4	2,147,058	1,740,053	67	4	16			87	0.00500				
WT (JMW007)	6 hr	1	2,145,677	1,511,288	59	41	11			111	0.00734	0.01224	0.00527	3.30	1.42
		2	2,431,609	1,610,373	180	80	27		3	287	0.01782				
		3	2,522,427	1,790,013	141	51	15		4	207	0.01156				
trm44-Δ tan1-Δ (JM119)	0 hr	1	2,553,264	1,713,750	101	26	10	2		137	0.00799	0.00782	0.00381	2.11	1.03
		2	1,847,577	1,292,496	26	6	8			40	0.00309				
		3	1,954,117	1,405,172	48	2	8			58	0.00413				
		4	2,028,146	1,377,183	87	14	6	3	2	107	0.00777				
		5	1,724,791	1,118,440	62	16	9			87	0.00778				
		6	2,279,391	1,451,951	101	26	6		2	133	0.00916				
		7	1,453,475	808,359	95	13	7		2	120	0.01484				
trm44-Δ tan1-Δ (JM119)	6 hr	1	1,996,874	1,273,668	1,181	1,868	75			3,124	0.24528	0.17440	0.03900	47.01	10.51
		2	2,507,487	1,630,090	1,142	1,492	77		2	2,711	0.16631				
		3	2,558,513	1,754,856	1,074	1,493	69			2,636	0.15021				
		4	1,508,822	1,004,566	585	692	41			1,318	0.13120				
		5	2,026,332	983,072	739	893	53			1,685	0.17140				
		6	1,332,707	657,766	540	598	57	2		1,197	0.18198				
trm44-Δ tan1-Δ (JM1251)	0 hr	1	1,353,146	104,710		1	6			7	0.00669	0.00840	0.00187	2.26	0.50
		2	782,805	73,836	2	2	2			6	0.00813				
		3	1,342,090	221,288	1	5	14		3	23	0.01039				
trm44-Δ tan1-Δ (JM1251)	6 hr	1	875,453	45,849		2				2	0.00436	0.00731	0.00540	1.97	1.46
		2	1,752,710	49,623	1	1				2	0.00403				
		3	518,307	29,528					1	3	0.01355				
trm44-Δ tan1-Δ (JM1251)	0 hr	1	646,958	87,650	3	1				4	0.00456	0.00511	0.00190	1.38	0.51
		2	466,026	69,244	3	2				5	0.00722				
		3	1,407,999	311,199	3	1	6			1	11	0.00353			
trm44-Δ tan1-Δ (JM1251)	6 hr	1	639,263	257,165	5	4	5		1	15	0.00583	0.00479	0.00270	1.29	0.73
		2	829,520	88,087	2	4				6	0.00681				
		3	229,523	57,791	1					1	0.00173				
trm44-Δ tan1-Δ (JM1251)	0 hr	1	126,218	48,985	4					4	0.00817	0.00589	0.00291	1.59	0.78
		2	99,674	43,564	2		1			3	0.00689				
		3	80,114	38,338		1				1	0.00261				
trm44-Δ tan1-Δ (JM1251)	6 hr	1	46,225	29,581	4	11	2			17	0.05747	0.07299	0.01949	19.67	5.25
		2	36,690	24,012	7	9				16	0.06663				
		3	29,879	18,973	5	9	4			18	0.09487				

Table S3

Strain	Time at 37	Replicate #	Total Reads	CCA	2 A's	3 A's	4 A's	5 A's	6 A's	7 A's	8 A's	9 A's	10 A's	11 A's	12 A's	SUM	% Reads with A tails	Average	StdDev	Relative Level	StdDev	
WT (JMW007)	0 hr	1	2,383,825	1,720,410	729	70	38	23								860	0.0500	0.03225	0.01239	1.00	0.38	
		2	2,836,577	2,215,590	552	45	19									616	0.0278					
		3	2,119,015	1,643,012	449	43										492	0.0299					
		4	2,147,058	1,740,053	318	39	13									370	0.0213					
WT (JMW007)	0.5 hr	1	3,131,139	2,387,937	982	114	31	23								1,150	0.0482	0.03535	0.00910	1.10	0.28	
		2	2,080,275	1,741,691	421	58										479	0.0275					
		3	1,863,204	1,561,183	414	51	12									477	0.0306					
		4	2,382,333	1,954,507	623	48	17									688	0.0352					
WT (JMW007)	1.5 hr	1	1,763,183	1,457,121	384	57										441	0.0303	0.03938	0.01100	1.22	0.34	
		2	1,807,474	1,480,671	682	70	12									764	0.0516					
		3	2,450,329	1,985,101	594	85	30	11								720	0.0363					
WT (JMW007)	3 hr	1	3,363,884	2,619,879	1,570	274	61	39	14	11	12					1,981	0.0756	0.05996	0.01456	1.86	0.45	
		2	2,774,037	1,456,810	511	99	31	15								656	0.0450					
		3	1,940,037	1,558,880	814	177	46	24	11							1,072	0.0688					
		4	2,238,661	1,788,351	665	157	46	23	11							902	0.0504					
WT (JMW007)	6 hr	1	2,145,577	1,511,288	788	322	84	56	26	21	17	27	13	12		1,366	0.0904	0.08663	0.01105	2.69	0.34	
		2	2,431,609	1,610,373	838	341	76	71	38	28	39	33	34	24	13	1,535	0.0953					
		3	2,522,427	1,790,013	785	278	65	48	27	30	23	22	26	14	10	1,328	0.0742					
trm44-Δ-tan1-Δ (JMW119)	0 hr	1	2,553,264	1,713,750	1,203	1,273	278	281	43	23	15					3,116	0.1818	0.12755	0.05463	3.95	1.69	
		2	1,847,577	1,292,496	538	344	66	74	14	15						1,051	0.0813					
		3	1,954,117	1,405,172	627	453	88	55								1,223	0.0870					
		4	2,028,146	1,377,183	476	419	99	107	17	12	11					1,141	0.0829					
		5	1,724,791	1,118,440	604	574	145	89	23	17						1,452	0.12982					
		6	2,279,391	1,451,951	590	664	168	117	26	11						1,576	0.10854					
		7	1,453,475	808,359	988	505	139	122	24	12						1,790	0.22144					
trm44-Δ-tan1-Δ (JMW119)	1.5 hr	1	1,425,638	1,078,057	2,793	1,421	269	172	58	71	24	19	12			4,839	0.4489	0.38305	0.09052	11.88	2.81	
		2	1,548,559	1,156,582	2,516	1,547	295	275	59	57	46	27	17	14		4,863	0.4205					
		3	1,786,720	1,413,013	2,256	1,106	31	372	63	54	36	22	14			3,954	0.2798					
trm44-Δ-tan1-Δ (JMW119)	3 hr	1	1,734,848	1,057,832	3,101	3,590	744	738	312	242	148	101	48	25	16	9,065	0.8569	0.44954	0.20747	13.94	6.43	
		2	2,421,152	1,830,979	5,053	2,999	524	423	174	177	80	42	33	20	11	9,536	0.5208					
		3	2,387,242	1,732,862	4,548	2,848	529	450	165	131	61	39	26	11		8,808	0.5083					
		4	2,731,860	2,208,457	3,957	1,905	342	271	83	65	50	33	20	12		6,738	0.3051					
		5	1,608,371	1,298,975	1,884	888	150	81	20	22	14					3,059	0.23549					
		6	2,026,332	983,072	6,442	3,391	697	608	360	369	377	355	373	205		6,726	0.33708					
		7	2,266,270	1,539,302	3,578	1,432	327	288	107	90	37	22	15			5,896	0.38303					
trm44-Δ-tan1-Δ met22-Δ (LY1729)	6 hr	1	1,996,874	1,273,568	9,590	7,295	1,591	1,433	737	610	492	445	425	369	242	23,238	1,8245	1,34262	0.28432	41.63	8.82	
		2	2,507,697	1,630,990	10,571	6,789	1,436	1,200	407	436	314	220	206	125	73	22,010	1,35249					
		3	2,558,513	1,754,856	10,450	5,906	1,284	1,096	553	438	386	357	355	266	256	21,436	1,2215					
		4	1,508,822	1,004,566	4,942	2,548	586	559	269	216	158	108	88	39		9,513	0.94698					
		5	2,026,332	983,072	6,442	3,391	697	608	360	369	377	355	373	205		13,177	1,34039					
		6	1,332,707	657,766	4,799	2,456	455	386	224	175	196	138	119	53		9,001	1,36842					
trm44-Δ-tan1-Δ met22-Δ (LY1729)	0 hr	1	3,146,850	2,196,850	1,645	277	60	44	22	22	10					2,080	0.0947	0.04629	0.02487	1.44	0.77	
		2	3,635,133	2,183,591	677	119	21									840	0.0299					
		3	3,230,696	2,407,540	610	102	31									766	0.0318					
		4	2,465,954	2,085,947	361	67	28									468	0.0224					
		5	2,010,837	1,391,668	457	79	15									561	0.04031					
		6	2,603,550	1,422,885	638	161	50	30	13							892	0.06269					
		7	2,376,861	1,420,369	437	119	27									600	0.04224					
trm44-Δ-tan1-Δ met22-Δ (LY1729)	1.5 hr	1	2,269,836	1,822,161	1,025	205	57	33	24	30	18	13	15	10		1,430	0.0785	0.08188	0.02716	2.54	0.84	
		2	2,289,474	1,606,948	1,351	230	56	46	27	25	16	14	12			1,777	0.1106					
		3	2,722,495	2,473,794	985	233	62	49	31	25	15					1,400	0.0566					
trm44-Δ-tan1-Δ met22-Δ (LY1729)	3 hr	1	3,199,484	2,334,115	1,928	685	209	150	65	77	63	33	28	18	12	3,268	0.1400	0.09905	0.02211	3.07	0.69	
		2	2,046,047	1,597,118	1,102	260	88	58	25	39	25	21	19	15		1,652	0.1034					
		3	1,973,749	1,509,434	1,016	300	100	66	35	25	24	26	19	10		1,621	0.1074					
		4	2,334,699	1,831,187	1,030	248	54	62	29	44	16	17	14			1,514	0.0827					
		5	2,457,998	1,944,618	1,423	183	38	28		10						1,682	0.08650					
		6	2,394,726	1,761,193	1,497	212	44	33								1,786	0.10141					
		7	2,411,522	1,634,700	906	168	32	24	17	19	10					1,176	0.07194					
trm44-Δ-tan1-Δ met22-Δ (LY1729)	6 hr	1	2,169,513	1,333,937	3,904	1,516	494	478	382	459	430	382	328	248	163	8,784	0.6585	0.44946	0.16903	13.94	5.24	
		2	2,242,084	1,450,986	3,721	1,566	592	545	381	476	490	450	313	279	147		8,960	0.6179				
		3	2,246,946	1,609,320	3,610	1,486	451	346	479	471	448	332	289	165		8,920	0.617					
		4	2,380,334	1,665,163	3,548	1,011	259	207	59	35	34	34	12			5,354	0.32347					
		5	2,371,125	1,609,933	3,297	883	231	187	135	137	127	99	72	26		5,194	0.32262					
		6	1,835,683	1,159,536	1,870	512	158	122	75	71	95	61	62	18		3,044	0.36252					
trm44-Δ-tan1-Δ xrn1-Δ (ISC850)	0 hr	1	2,547,502	1,733,200	677	181	29									904	0.05216	0.08543	0.02958	2.65	0.92	
		2	1,887,586	1,111,647	840	169	24									1,060	0.09535					
		3	2,148,658	1,234,743	1,057	218	32									1,343	0.10877					
trm44-Δ-tan1-Δ xrn1-Δ (ISC850)	3 hr	1	2,275,988	1,607,613	891	205	34	19		11						1,160	0.07216	0.06702	0.01467	2.08	0.45	
		2	2,052,082	1,618,636	635	146	24		12							817	0.05047					
		3	2,214,119	2,023,748	1,464	276	72	53		13	11					1,613	0.07842					
trm44-Δ-tan1-Δ xrn1-Δ (ISC850)	6 hr	1	2,327,188	1,784,834	1,311	262	47	21		16						1,657	0.09284	0.09601	0.00507	2.98	0.16	
		2	2,706,605	1,890,755	1,353	493	44	36								1,926	0.10186					
		3	3,057,414	1,203,748	1,464	276	72															

Table S4

Strain	Time at 37	Replicate #	Total Reads	CCAA												% Reads with A tails	Average	Stdev	Relative Level	Stdev	
				CCA	2A's	3A's	4A's	5A's	6A's	7A's	8A's	9A's	10A's	11A's	12A's						
WT (JMW007)	0 hr	1	2,383,825	1,720,410	729	70	38	23								860	0.0500	0.03225	0.01239	1.00	0.38
		2	2,836,577	2,215,590	552	45	19									616	0.0278				
		3	2,119,015	1,643,012	449	43										492	0.0299				
		4	2,147,058	1,740,053	318	39	13									370	0.0213				
WT (JMW007)	6 hr	1	2,145,677	1,511,288	788	322	84	56	26	21	17	27	13	12		1,366	0.0904	0.08663	0.01105	2.69	0.34
		2	2,431,609	1,610,371	838	341	76	71	38	28	39	33	34	24	13	1,535	0.0953				
		3	2,522,427	1,790,013	785	278	65	48	27	30	23	22	26	14	10	1,328	0.0742				
trm44-Δ tan1-Δ (JMW119)	0 hr	1	2,553,264	1,713,750	1,203	1,273	278	281	43	23	15					3,116	0.1818	0.12755	0.05463	3.95	1.69
		2	1,847,577	1,292,496	538	344	66	74	14	15						1,051	0.0813				
		3	1,954,117	1,405,172	627	453	88	55								3,223	0.0870				
		4	2,038,146	1,377,183	476	419	99	107	17	12	11					1,141	0.0829				
		5	1,724,791	1,118,440	604	574	145	89	23	17						1,452	0.12982				
		6	2,279,391	1,451,951	590	664	168	117	26	11						1,576	0.10854				
		7	1,453,475	808,359	988	505	139	122	24	12						1,790	0.22144				
trm44-Δ tan1-Δ (JMW119)	6 hr	1	1,996,874	1,273,668	9,590	7,295	1,591	1,433	737	619	492	445	425	369	242	23,238	1.8245	1,34262	0.28432	41.63	8.82
		2	2,507,487	1,630,090	10,871	6,780	1,436	1,200	407	438	314	220	206	125	73	22,070	1.3539				
		3	2,558,513	1,754,856	10,450	5,905	1,284	1,096	553	438	386	357	355	356	256	21,436	1.2215				
		4	1,508,822	1,004,566	4,942	2,548	586	559	269	216	158	108	88	39		9,513	0.94698				
		5	2,026,332	983,072	6,442	3,391	697	608	360	369	377	355	373	205		13,177	1.34039				
		6	1,332,707	657,766	4,799	2,456	455	386	224	175	196	138	119	53		9,001	1.36842				
trm44-Δ tan1-Δ (JMW1251)	0 hr	1	1,353,146	104,710	50	6										56	0.05348	0.03620	0.01508	1.12	0.47
		2	782,805	73,836	17				2							19	0.02573				
		3	1,342,090	221,288	57	6	2									65	0.02937				
trm44-Δ tan1-Δ (JMW1251)	6 hr	1	875,453	45,849	16											16	0.03490	0.02738	0.00738	0.85	0.23
		2	1,752,710	49,623	10											10	0.02015				
		3	518,307	29,528	6	2										8	0.02709				
trm44-Δ tan1-Δ (JMW316)	0 hr	1	646,958	87,650	21	5										26	0.02966	0.07007	0.07064	2.17	2.19
		2	466,624	69,244	94	11										105	0.15164				
		3	1,407,999	311,199	72	11	5	2								90	0.02892				
trm44-Δ tan1-Δ (JMW316)	6 hr	1	630,263	257,165	78	9	3	3	3							96	0.03733	0.06838	0.06704	2.12	2.08
		2	829,520	88,087	111	7	2	3	3	2						128	0.14531				
		3	229,523	57,791	13											13	0.02249				
trm44-Δ tan1-Δ (JMWS61)	0 hr	1	126,218	48,985	73	23	6	4			2					108	0.22048	0.14055	0.07024	4.36	2.18
		2	99,674	43,564	10	27	3	9								49	0.11248				
		3	80,114	38,338	13	15	2	4								34	0.08868				
trm44-Δ tan1-Δ (JMWS61)	0 hr	1	46,225	29,581	46	46	10		3							105	0.35496	0.35550	0.01845	11.02	0.57
		2	36,690	24,012	42	30	6	3								81	0.33733				
		3	29,879	18,973	37	25	3	4	2							71	0.37422				

Table S5

Northern Probes used in Fig. 1B, Supplementary Fig. 7A	Sequence
mascRNA	ggccccctt

MEN β tRNA-like small RNA aaccggccggccaaaggctgtttggac